Addis Ababa University

Addis Ababa Institute of Technology

School of Graduate Studies

School of Mechanical and Industrial Engineering

OPTIMIZATION OF MACHINING PARAMETERS IN DRILLING HYBRID SISAL-COTTON FIBER REINFORCED POLYESTER COMPOSITE

A Thesis Submitted to the Graduate School of Addis Ababa University in Partial Fulfillment of the Requirement for the Degree of Masters of Science

In

Mechanical Engineering (Manufacturing Engineering)

By: **Nurhusien Hassen**

Advisor: **Dr. Desalegn Wogaso**

Addis Ababa, Ethiopia

July 2021

Addis Ababa University

Addis Ababa Institute of Technology

School of Graduate Studies

School of Mechanical and Industrial Engineering

OPTIMIZATION OF MACHINING PARAMETERS IN DRILLING HYBRID SISAL – COTTON FIBER REINFORCED POLYESTER COMPOSITE

By: Nurhusien Hassen

Submitted in accordance with the requirements for the degree

MASTER OF SCIENCE(M.Sc.)

Approved by Board of Directors:

Dr. Dessalegn Wogaso	_____	_____
Advisor	Signature	Date
_____	_____	_____
Internal Examiner	Signature	Date
_____	_____	_____
External Examiner	Signature	Date
Dr. Yilma Tadesse	_____	_____
Chairman of the School	Signature	Date

DECLARATION

Addis Ababa University

School of Graduate Studies

This is to certify that the thesis prepared by **Nurhusien Hassen**, entitled: ***Optimization of Machining Parameters in Drilling Hybrid Sisal – Cotton Fiber Reinforced Polyester Composite,*** do hereby declare this thesis is my original work and that it has not been submitted partially or in full for a degree in any university/ institution, which complies with the regulations of the university and meets the accepted standards concerning originality and quality.

Name: Nurhusien Hassen

Place: Addis Ababa, Ethiopia

Signature:_____

Date: _____

Advisor: Dr. Desalegn Wogaso Signature:_____ Date: _____

Head of School: Dr. Yilma Tadesse Signature:_____ Date: _____

ACKNOWLEDGEMENT

First and foremost, I want to express my gratitude to The Almighty GOD for allowing me to begin and complete my thesis work in this difficult situation.

I am grateful to my thesis advisor, Dr. Desalegn Wogasso, Assistant Professor, School of Mechanical and Industrial Engineering, for his genuine guidance and checkups in the thesis writing process. I'm also grateful to Dr. Yilma Tadesse, the Dean of the School of Mechanical and Industrial Engineering, for his assistance and cooperation. I appreciate the support of Addis Ababa University's School of Mechanical and Industrial Engineering members.

I would like to express my sincere thanks to my friends who work in KADISCO paints and METEC for their help during the fabrication and experimental work on my research studies. And also I'm thankful to Addis Ababa Science and Technology University's Shop Technician who helped me in the surface roughness measurement using Zeta 20 Profilometer at the restricted time due to COVID 19.

Finally, I'd like to express my gratitude to all of the people who assisted me in my research work at various locations from beginning to end.

ABSTRACT

As compared to metals, composite materials machining is a challenge because the cutting tool needs to move through the matrix and fiber alternately, which have various properties. The objective of this work is to optimize the machining parameters in drilling hybrid sisal-cotton fiber reinforced polyester composite (HSCFRPC) to reduce the hole roundness error and surface roughness using Taguchi's method. The influence of machining parameters such as spindle speed, drill diameter, and feed rate on the surface roughness and roundness error of HSCFRPC during the drilling process on the vertical CNC milling machine have been analyzed using the methods of Taguchi's design of experiment. A series of experiments based on L_{16} orthogonal arrays were established with different feed rates (10, 15, 20, 25 mm/min), spindle speeds (600, 900, 1200, 1600rpm), and drill diameter (6, 7, 8, 10mm). The measurement of roundness error and surface roughness have been carried out using ABC digital caliper and Zeta 20 profilometer respectively. The experimental values are gathered and analyzed using the MINITAB 19 commercial software program. To create a connection between the chosen drilling parameters and the quality attributes of the drilled holes, linear regression equations have been established. Signal to noise (S/N) ratio analysis and analysis of variance (ANOVA) were performed to identify the rank, percentage contribution and optimum values of these machining parameters such as spindle speed, drill diameter, and feed rate to reduce the roundness error and surface roughness. Based on the analysis the best combination of the optimum machining parameter values (1600rpm, 25 mm/min, and 6mm) are selected to reduce both roundness error and surface roughness of the composite. Finally, verification of the recommended machining parameters have been achieved and the values of roundness error and surface roughness obtained are 0.1mm and 64.8µm Ra respectively, which satisfies the objective of lowest roundness error and surface roughness. The verification result shows that the recommended machining parameter values to reduce roundness error and surface roughness based on Taguchi's analysis were precise and fitted to the optimum values.

Key Words: *Drilling, Roundness Error, Surface roughness, Machining Parameters, Taguchi's method, Regression analysis, S/N ratio, ANOVA.*

TABLE OF CONTENTS

NOMENCLATURE

M_f	Mass fraction of fiber material (gm.)
M_m	Mass fraction of matrix material (gm.)
M_c	Mass fraction of composite material (gm.)
M_{cf}	Mass fraction of cotton fiber (gm.)
M_{sf}	Mass fraction of sisal fiber (gm.)
$\boldsymbol{\rho}$	Density (g/cm^3)
ρ_m	Density of matrix material (g/cm^3)
ρ_f	Density of fiber matrix material (g/cm^3)
ρ_c	Density of composite material (g/cm^3)
V_f	Volume of fiber (cm^3)
V_m	Volume of matrix (cm^3)
V_C	Volume of composite (cm^3)
V_{Ca}	Volume of catalyst (cm^3)
D_{max}	Maximum diameter (mm)
D_{min}	Minimum diameter (mm)
S	Spindle speed (rpm)
F	Feed rate (mm/min)
D	Drill diameter (mm)
R_a	Arithmetic mean deviation (µm)
R_q	Root mean squared (µm)
R_{pv}	Maximum valley depth below the mean line (µm)
R_p	Maximum peak height above the mean line (µm)

R_v	Average distance between the highest peak and lowest valley (µm)
R_{sk}	Skewness (µm)
R_z	Ten-point mean roughness (µm)
R_{ku}	Kurtosis (µm)
R_E	Roundness error (mm)
S_R	Surface roughness (µm)

LIST OF ACRONYMS AND ABBREVIATIONS

Adj SS	Adjusted sum of squares
ANOVA	Analysis of variance
ASTM	American society of testing material
HSCFRPC	Hybrid sisal-cotton fiber reinforced polyester composite
CNC	Computer numerical control
NFRP	Natural fiber reinforced polymer
FRP	Fiber-reinforced polymer
UTM	Universal testing machine
HSS	High-speed steel
RBFN	Radial basis function network
OA	Orthogonal array
MPa	Mega pascal
Ne	Number English
ml	Milliliter
Sec	Second
GPP	General Purpose polyester
KJ/m	Kilo joule per meter
Rpm	Revolution per minute
DOE	Design of experiment
DF	Degree of freedom
SS	Sum of squares
Seq SS	Sequential sum of squares
S/N	Signal to noise ratio

SN	Signal to noise
F-value	Variance
P-value	Calculated probability
µm	Micrometer
min	Minute
METEC	Metals and Engineering Corporation
10x	ten times
3D	Three Dimensional
Eq.	Equation
Fig.	Figure
SD	Standard Deviation
S/N_L	Lower the better signal to noise ratio
PLC	Diamond-like carbon
PCD	Polycrystalline diamond
PCBN	Poly Crystalline Cubic Boron Nitride
PMHSS	Powder Metallurgical High-Speed Steel

LIST OF FIGURES

LIST OF TABLES

CHAPTER ONE

INTRODUCTION

1.1 Introduction

This chapter introduces the content, main focus area, and structure of the research. It covers the background of the study, statement of problems, objectives of the study, scope of the research, significance of the study, and the organizations of the entire thesis.

1.2 Background of the Study

To address the inherent defects in polymer materials, natural fibers have various significance as reinforcement. There have been a steady interest in using natural fibers to polymer composites in recent years and in manufacturing goods based on them to provide alternative materials that are energy-efficient, economical, and environmental.

The use of automotive parts based on plant fiber (sisal, cotton, flax, hemp, etc.) such as trim parts, shelves, different panels, and brake shoes attracts automotive industries worldwide due to its weight reduction of about 10 percent, 80 percent energy efficiency, and 5 percent component cost[1]. In the automotive industry, hybrid sisal-cotton fiber reinforced polyester composites have several applications. For instance, the Mercedes Benz (C-Class) rear panel shelf is made of sisal-cotton fiber and 95% recyclable vehicles (Daimler Chrysler or M-B Travego Coach) are made of sisal, flax, coir, hemp, and cotton fiber [2-3]. This material has very low weldability and can therefore be bolted to connect the material.

Drilling is the best common machining process used for the creation of circular profiles for fitting, followed by fasteners [4-5]. There are numerous kinds of machining processes. Drilling operations on composite laminates are significant that have useful results for fastening with other materials [6]. Several defects such as delamination, inter-laminar cracks, and fiber pull-out can result from the drilling process on the fiber-reinforced composites [7]. Such inconveniences are capable of affecting the mechanical material properties of the components generated, thereby reducing consistency.

Hybrid composite machining with minimal roundness error and surface roughness are a challenge for one and all of the composite sector-related industries. Therefore, to achieve good surface finish characteristics and quality goods, addressing these problems has a lot of significance.

Roundness error and surface roughness are a degree of the surface quality of a product and are an influence that have a high effect on the products. To minimize roundness error and surface roughness, this research work will therefore aim at examining the consequence of machining (drilling) parameters on the hybrid sisal-cotton fiber reinforced polyester composites. The literature reviews suggest that the consequence of machining parameters in hybrid composites have been studied in only a few research papers and there is no work on the influence and optimization of drilling machining parameters in hybrid sisal-cotton fiber reinforced polyester composites drilling [7].

Here, an attempt has been made to establish the application of Taguchi's Method to reduce roundness error and surface roughness to improve the quality of the surface characteristics and mechanical performance of drilled hybrid sisal-cotton fiber reinforced polyester composites that are drilled on the CNC milling machine.

1.3 Problem Statement

During the drilling of various fiber-reinforced composite laminates, the consistency and reliability of the holes acquired are very various from drilled metals. Owing to the abrasive design, heterogeneity, and anisotropy of the NFRP composite materials, making a hole in metal surfaces are uniform and more constant than the drilled fiber-reinforced polymer (FRP) composite material surfaces under similar circumstances.

Due to the poor machinability properties of fiber-reinforced polymer composite, there are a lot of problems encountered during the drilling operation of these composite materials. Among the problems surface roughness and roundness error are the main problems encountered during the drilling process of fiber-reinforced polymer composite.

Furthermore, the poor machinability of NFRP is due to the combination of the poor thermal conductivity of the resin matrix, as well as the toughness and abrasiveness properties of some

NFRP composites. Several severe drilling-induced damage results from the effects of these properties on a drilled composite, including roundness error, surface roughness, delamination, crack growth, stress concentration, lint formation, drill edge chipping, and excessive wear, chipping, uncut and pinched fiber, sintering, or burning of the matrix and detachment [62].

Among the most main defects on drilled composite materials surface roughness and roundness error are the major problems. Roundness error is well-defined as the key sort of laminated composite failure, whereby the diameter deviation from the drill-hole diameter. Meanwhile, the surface roughness within the estimated length is defined as the mean deviation of the roughness profile from the midline. In tribology, rough surfaces generally wear out faster and have higher coefficients of friction than smooth surfaces. Roughness is often an indicator of a mechanical component's performance, as irregularities in the surface can form nucleation sites for cracks or corrosion. In a drilled hole, roughness is a very important quality because crack propagation, creep, wear, fatigue and corrosion mechanisms depend on it [62].

Hence, this research presents the optimization of machining parameters such as spindle speed, feed rate, and drill diameter on surface roughness and roundness error using Taguchi's method of regression, S/N ratio, and ANOVA analysis based on obtained response values (surface roughness and roundness error) of L_{16} orthogonal array matrix experimental data with different spindle speeds, feed rates, drill diameters during the drilling process of hybrid sisal-cotton fiber-reinforced composite material to reduce surface roughness and roundness error problems.

1.4 Objectives

1.4.1 General Objectives

The general objective of this research is to optimize the drilling parameters of hybrid sisal-cotton fiber reinforced polyester composite to reduce the surface roughness and roundness error of this composite material.

1.4.2 Specific Objectives

Through the following highlighted objectives, the stated main objectives will be implemented. Therefore, the specific objectives of the study are to:

- Fabricate hybrid sisal-cotton fiber reinforced polyester composite.
- Measurement of roundness error and surface roughness drilled hybrid sisal-cotton fiber reinforced polyester composite.
- Optimize the important machining parameters in the drilling process of HSCFRPC.
- Verify the recommended optimum machining parameters in the drilling operation of HSCFRPC by checking the validation of recommended optimum values experimentally.

1.5 Scope of the Research

This study focuses on the optimization of machining parameters such as spindle speed, feed rate and drill diameter in drilling hybrid sisal-cotton fiber reinforced polyester composite to reduce roundness error and surface roughness.

Different constituents were used to fabricate the composite specimen. These constituents include hybrid sisal-cotton fiber and polyester resin matrix. And the methods used to manufacture the composite material was hand lay-up method.

The drilling operation for this study were performed by GSK CNC milling machine based on the Taguchi's L_{16} orthogonal array with different spindle speed, feed rate and drill diameter. The roundness error and surface roughness of the drilled holes were measured using HOLEX ABC slide digital caliper and ZETA 20 profilometer respectively.

Finally the regression analysis, S/N ratio, and ANOVA were performed to identify the optimum machining parameter values to reduce both roundness error and surface roughness of the drilled holes.

1.6 Significance of the Study

Among the principal machining activities, drilling plays an important role to assemble different parts of fiber-reinforced polymer composites in a machine by using bolt and nut because the fiber-reinforced polymer composite materials can not be welded effectively.

Roundness error and surface roughness have been reported on FRP composite materials as the most critical drilling-induced damage. Consequently, the disclosure of optimal drilling parameters and conditions under which surface roughness and roundness errors could be reduced and the proposed Taguchi methods have great academic and industrial relevance for the fiber-reinforced polymer composites machining. The techniques are capable of predicting minimum roundness error and surface roughness, and critical spindle speed, feed rate, and drill bit diameter, which will effectively minimizes surface roughness and roundness error of the holes in drilling HSCFRPC. This study is also very important for fiber-reinforced polymer composite drilling researchers, designers, producers (manufacturing companies), and users of the drilling process.

1.7 Limitations

There were many obstacles while conducting this research work, the major obstacles faced include, first, it was hard to obtain a journal and a book about hybrid sisal-cotton fiber reinforced polyester composite, second CNC drilling machine was not available in Ethiopia due to this problem drilling of HSCFRPC was performed using CNC milling machine, finally obtaining 3D profilometer to measure surface roughness of internal walls of the hole was a challenge.

1.8 Organization of the Thesis

This study focuses on the optimization of machining parameters in drilling HSCFRC. The contents of this thesis are organized and discussed in five different chapters. The outline of the thesis is structured as follows in Table 1.1:

Chapter 1: Introduces the background of the study, problem statement, Objective of the study, the scope of the research, significance of the study and its limitation of the study.
Chapter 2: Contains a literature review to provide the research trend and gap of the main points of this thesis. It presents the hybrid fiber-reinforced polymer composites, the application of fiber-reinforced composites, and machining of composites carried out by different investigators.
Chapter 3: Provides information about the materials and experimental methods used in the thesis are discussed in this chapter. This includes matrix and fiber materials, methods of sample preparation, experimental methods and techniques, the process of drilling, and finally, measurement of roundness error and surface roughness of the hybrid sisal-cotton fiber reinforced polyester composite laminate.
Chapter 4: Presents the result and discussion on the roundness error, surface roughness, and verification of recommended parameters using Taguchi's method of regression analysis, signal to noise ratio, and analysis of variance.
Chapter 5: Provides conclusions based on the experimental study and recommendations for future work.

Table 1. 1: Organization of the thesis

CHAPTER TWO

LITERATURE REVIEW

2.1 Introduction

This literature review relies on the thesis title and explores extensively related works, fiber-reinforced polymer composites, the application of fiber-reinforced composites, hybrid fiber-reinforced polymers, types of fiber-reinforced composite, composite matrices(binders), and, finally, drilling of fiber-reinforced polymer composite.

2.2 Composite Materials

2.2.1 Introduction

Composite materials are composed of two main constituents which are matrix and reinforcing materials. Composite materials include multicomponent substances created by combining several materials artificially to get qualities that a single component cannot achieve on its own. The ideal characteristic and application of modern composite materials, which are largely mechanical, is fibers or particles surrounded by another matrix material. Composite materials are made up of multiple layers of components that give them the unique characteristics of a composite material with a specified application. Fibers without a matrix can't withstand a load, but when the matrix is in them, fibers of various compositions are joined by the matrix and give them unique characteristics. Reinforcing materials are often designed to absorb a high load while also providing desired characteristics [2].

2.2.2 Matrix Materials (binders)

The load-carrying capacity of reinforcing fibers in FRCs is determined by matrix materials. These materials, also known as resins, are an important part of any FRC and affect its overall performance. They have three key functions in the composite structure and are listed below [2]:

(i) Used to transfer mechanical stresses from the surface of a composite to its reinforcement.
(ii) The composite's reinforcing fibers' adhesion.
(iii)Act as abrasion and chemical protection of composite surfaces.

Binders are necessary because they ensure interfacial bonding of the fibers, which determines the mechanical characteristics of FRC. Modulus and strain, t ensile strength, compression strength

and modulus, impact resistance, notch sensitivity, ease of availability, glass transition temperature, ease of availability, and price are all important factors to consider when choosing a resin device. Resins cover approximately 40–50% of the composite weight, but they contribute less to the overall composite cost and are mainly judged on the tensile strength and of the material [8]. According to the chemical nature of binders, they can be divided into two classes:

(i) Thermosets: These are polymers that degrade irreversibly at temperatures above 200 degrees Celsius. They may either be molded to their final form or used as adhesives directly. Amino, polyester, phenolic, and epoxy are some of the most popular thermosets used in manufacturing.

(ii) Thermoplastics: These are polymers that, even after curing, can be re-melted into a liquid state. They are durable, resilient, and corrosion resistant, but they need higher curing temperatures. The most frequently found thermoplastic polymers in practice are polyethylene (PE), polystyrene (PS), polyvinyl chloride (PVC), and polypropylene (PP).

2.2.2.1 Epoxy resins

ECHOCH2 is a generalized reactive group that includes thermosetting matrices composite. These polymers, also known as polyepoxides, are the most widely used binders in the reinforcement of composite due to a variety of beneficial properties. Metal coatings, structural adhesives, electrical insulations, structural adhesives, binders, and encapsulates are a few of the applications. They have a special range of properties not found in other thermoset resins. Nowadays, most epoxy resins are made from petroleum products, but some are made from natural sources like glycerol. Most widely used reinforcing fibers, such as carbon, basalt, fiberglass, aramid, and aramid are compatible with it [8].

The mechanical strength of flax and hemp fiber composites was used to assess the supremacy of epoxy resin matrices in research performed by Hepworth and Bruce [10]. At an 80 percent volume fraction of flax fibers in epoxy resins, the results suggested the output of a composite with a mean modulus of 378 MPa and a mean stiffness of 26 GPa. Similar fiber combinations of phenolic resin, on the other hand, resulted in a weak composite with a mean modulus of 27 MPa and a mean stiffness of 3.7 GPa.

General properties of Epoxy resins [8]

(i) Excellent adhesion properties to other materials.
(ii) High resilience and toughness.
(iii) Low shrinkage during the curing process.
(iv) Effective electrical insulation.
(v) Chemical and solvent resistance.
(vi) Poisonous quality and toxicity.
(vii) Low production or acquisition cost.
(viii) The product has a long shelf life.
(ix) Wide use due to its compatibility with a wide range of substrates.

2.2.2.2 Vinyl esters

This is a thermosetting plastic polymer that is produced by esterifying an epoxy resin with an unsaturated monocarboxylic acid. It's a reliable matrix that's widely used in the composites industry. It has won preference over other composite matrices in marine environments, oil, and infrastructure industries due to its excellent strength, corrosion resistance, and water absorption resistance [11].

Vinyl esters have a higher tensile strength than polyesters and epoxy resins, as well as a lower resin viscosity (approximately 200 cps) than polyester (approximately 500 cps) and epoxy (approximately 900 cps). It's often used in the production of FRC tanks and vessels, as well as in the fabrication of tanks, pipes, and process equipment. It can be applied by hand or sprayed on a one-time basis [11].

General properties of vinyl esters

(i) The ability to withstand extreme temperatures.
(ii) Excellent solvent resistance
(iii) High resistance to corrosive substances like alkalis, acids, and oxidizing agents.
(iv) Excellent tensile strength

2.2.2.3 Polyester resins

Another effective adhesive used in composite binding is a polyester resin. Glycols, dicarboxylic acids, and monomers make up this substance. The glycols and dicarboxylic acids react together

to form an ester in the presence of high heat (up to 430^0F) and a long exposure period (usually 14–24 hours). This is known as the esterification reaction [9].

UPE resins (unsaturated polyester resins) are used in several consumer and industrial applications. Because of their ability to positively affect the overall mechanical properties of FRCs by stronger interfacial bonding, it is widely used for reinforcement adhesion in FRCs. When polyester resins are reinforced with structural fibers like glass and natural fibers, strong composite material is created [9].

General properties of polyester resins

The mechanical properties of polyester resins are shown in Table 2.1. A comparison of polyester and epoxy resins in a hybrid composite of hemp and jute fibers was performed by Girisha, Anil, and Akash in their study. The findings of this study demonstrated that polyester resins outperformed epoxy resins in terms of tensile, structural, and impact strength of the composite [9].

Table 2. 1: Unsaturated polyester resins' mechanical properties [10].

Property	Unit
Density	1200 (kg/m^3)
Thermal conductivity	0.17 (W/m.oC)
Tensile strength	70.3 – 103 (MPa)
Modulus of elasticity	2.06 – 4.41 (GPa)
Fracture toughness	0.6 (M.Pa.m$^{0.5}$)

2.2.2.4 Comparison of composite matrices

Adhesive quality: Epoxy resin has a lower volumetric shrinkage than its ester counterparts, making it a stronger adhesive. It is highly favored for use in NFRCs and SFRCs applications as a result of this property [8].

Resin Structure: Tensile strength and stiffness of a post-cured epoxy resin are usually double those of a non-post-cured vinyl ester or polyester [8].

Tensile strength: Tensile strength and elastic modulus of polyester and vinyl ester resins are higher than epoxy resins. However, as shown in Figures 2.5 and 2.6, the property of an epoxy resin can be easily enhanced by using suitable reinforcing fibers in a composite laminate. Epoxy had the highest tensile strength of 8 MPa and the highest tensile modulus of approximately 3.5 GPa after a shorter period of 5 hours at a higher temperature of 176^0F. After 7 days at 68 degrees Fahrenheit, the epoxy tensile modulus increased [8].

Shrinkage: Vinyl esters and polyesters have a volumetric shrinkage propensity of about 7%, whereas epoxies have a much lower value of 2%. Epoxy resins are more stable than their ester equivalents because of this [8].

Microcracking and Fatigue resistance: Polyesters and vinyl esters, which are comparatively more brittle resins, have lower failure strain levels. As a result, the component's fatigue tolerance was low, and cracks were easily formed, leading to component failure. Epoxy resin has a better ability to withstand cyclic stresses that cause fatigue failure, which is why it is used more often in aircraft applications [8].

Water resistance: To some degree, all resins absorb water, increasing composite weight. The effect of water on composite binders' stability and shelf life is critical when determining their shelf life. If polyesters and vinyl esters can only retain about 65 percent of their initial shear strength after water penetration, epoxy resin can retain a whopping 90 percent. Epoxy resins are thus well suited to marine applications and other applications where water intrusion is a common occurrence [8].

2.2.3 Reinforcement Materials

Reinforcement materials are used to increase rigidity and minimizes the propagation of cracks during their mechanical applications. Particularly they increase the mechanical strength

properties of the matrix and most of the time they are stronger, harder, and stiffer than the matrix material. The reinforcement materials are classified into four elementary categories: Fibers, fillers, particulates, and flakes [11].

Flakes have two-dimensional geometry in two directions with stiffness and strength. They form good composite material when poured into a plastic or glass. Among these materials aluminum, mica and silver are the most commonly used flakes.

Fillers are powders or particles poured into a certain material to develop and modify composites' mechanical properties. Fillers are added to enhance or improve properties such as electrical resistivity, thermal conductivity, wear resistance, friction, and flame resistance.

Particulates are small particles in the composite materials less than 0.25μm, cubes, hollow spheres, platelets. The particulate delivers the required properties of materials, and the matrix material used as a binding medium important for applications of the structural materials used as particulates are copper, lead, tungsten, chromium, and molybdenum.

Lastly, fiber is a string, filament, or rope constituent of the composite materials. The shape of the fiber can be square, circular, or cylindrical. There are different natural and synthetic fibers widely used in the manufacturing of composites. Materials used as fibers are sisal, glass, cotton, aramid, carbon, boron, silicon carbide, etc.

2.3 Fiber Reinforced Polymer (FRP) Composites

The interaction of science (physics, materials, and chemistry) and engineering knowledge has been credited with recent advances in the field of composite materials manufacturing (mechanics and manufacturing) [12]. The deep and thorough study of fiber-reinforced polymer (FRP) composites is an interdisciplinary practice [13]. FRP fiber composites of different properties for various applications were produced as a result of the search for high corrosion resistance materials and efficient load-bearing capability structures in the areas of materials science and engineering, respectively. The mechanical properties of Composite materials are essential during the manufacturing processes and service because they decide the composites' functionality, performance, and workability.

The FRP composite material is thought to be a superior material with improved durability since it is made up of two or more materials that are unsolvable in each other and have unique chemical and physical properties [14]. It is shaped into a single-ply by combining fiber and matrix, which act as reinforcement and binder, respectively. The reinforcement is often bonded in between matrices, as shown in Fig.2.3.

A composite material is a heterogeneous solid made up of two or more distinct individual materials joined by a mechanical bond. Although each constituent material within the composite can behave differently without the bond, the resulting properties of composite material are the sum of its individual materials' considerable variation [15].

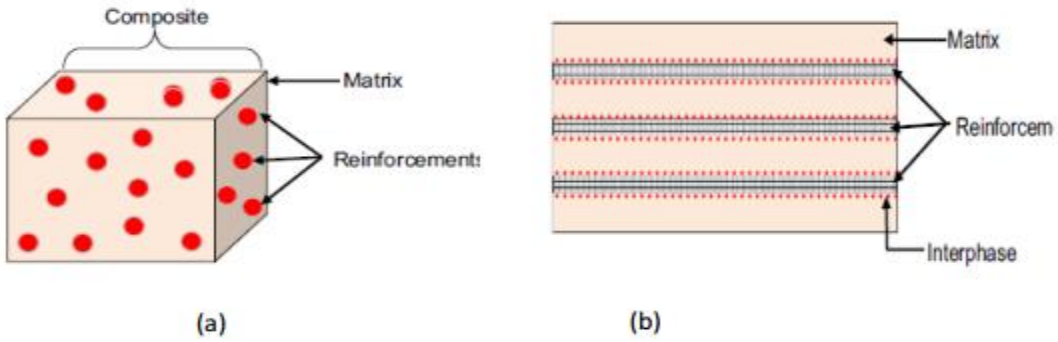

Figure 2.1: Picture diagram of composite (a) Reinforcement and matrix illustration; (b) Interfacial borders [15].

This indicates that both the reinforcement and the matrix bear the applied loads on the composite, but that the reinforcement, as a heavier, stronger constituent and chief load carrier, carries the load while the binder (matrix) disperses the load to the fiber (reinforcement); acts as a stress transfer component, holds the fibers securely and prevents the fiber surface from physical (fracture) and chemical (abrasion) damage [11]. The attributes of these two key ingredients, their boundaries (interfaces), and microstructures, all have an impact on the performance of FRP composites.

The production of composite materials became necessary to overcome the individual limitations of conventional materials (metals and alloys). Given that different applications necessitate the use of various mechanical properties. The extent of property modification that composite materials provide immediately makes them an attractive option in manufacturing technology. Fiber-reinforced composites (FRCs), which have a special level of specific stiffness and strength, as well as low weight, are the most common forms of composite materials [16]. They are usually embedded by stiff fibers of different materials of selection, with the main goal of achieving a material with high rigidity and modulus (implies high strength and stiffness to weight ratio). Furthermore, the embedded fibers are structured in such a way that they can work together in

synergy. Fiber-reinforced composites are made up of two main components: reinforcement and matrix.

Reinforcements: are single-material filaments that make up the composite's structure. They are usually organized concisely to achieve the required properties of the final composite material. The reinforcement usually fills 10 to 70 percent of the composite matrix volume, It can be obtained naturally or by synthetic processing. However, the most commonly used reinforcement fibers in structural parts are biomass, aramid, and fiberglass [16].

Matrix is the gluey portion of the composite, which is usually viscous but thin. It performs three main functions within the composite material: mechanical bonding of embedded reinforcements, the transmission of mechanical stress from composite polymer to its reinforcements, and protection of the surface of the composite from abrasion or chemical attack. The matrix is applied to the interlayer borders of the reinforcing fibers for binding purposes. Composite matrices include polyester resins, epoxy resins, vinyl esters, and polycaprolactone[16].

Any fiber-reinforced composite's efficiency is normally determined by a variety of factors, including: (1) the component materials' property characteristics. (2) the continuity of the matrix-reinforcement interfacial bonding; hence, the importance of interfacial interaction and the orientation of individual components are denoted [16], as depicted in Figure 2.4. The mechanical characteristics of the reinforcing fibers and the adhesion strength of the matrix-fiber interface are governed by the properties of the reinforcing fibers and the adhesion strength of the matrix-fiber interface, such as the off-axis strength and impact strength of FRCs, whereas the durability of the adhesive matrix is driven by other key properties, such as thermal stability and chemistries [17]. Fiber reinforced composites are commonly used in applications that require a high strength-to-weight ratio and rigidity, such as automotive, aerospace, structural industries, and a variety of other consumer and technological applications.

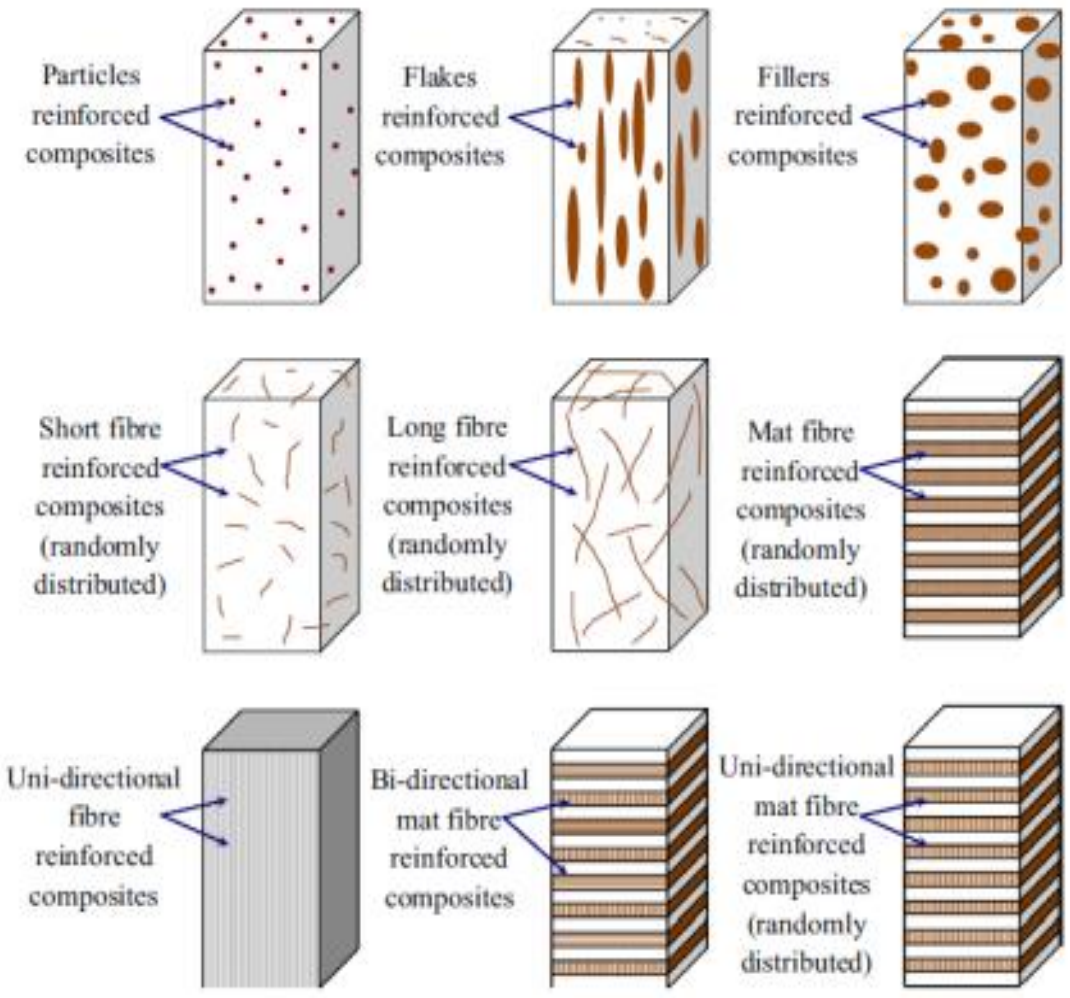

Figure 2.2: Types of reinforcements; displaying organization of their fibers, fillers, and particles within various composites [15].

Fiber-reinforced composites are becoming the required and preferred material structure in many industrial applications today. They have greater electromagnetic clarity, part count reduction, durability, rigidity, design versatility, lightweight, strength properties, mechanical damping, strength properties, and chemical, thermal, corrosion, and wear resistance than conventional metal engineering materials [14]. These improved properties and growing application of fiber-reinforced composites have stressed the need to recognize their machinability to continue to develop their functionality.

2.3.1 Types of Fiber-Reinforced Composites

Fiber-reinforced composites are usually classified according to the type of reinforcement (fibers), rather than the matrix. Each type's naming convention is based on the source of reinforcement. As a result, there are two types of fiber-reinforced composites: natural fiber-reinforced composites (NFRC) and synthetic fiber-reinforced composites (SFRC).

2.3.1.1 Natural fiber-reinforced composites

Natural fiber-reinforced composites, also known as bio-composites or green composites, are composites that have embedded bio-fiber reinforcements. The fiber reinforcements in this form of composite come from natural sources such as plants, minerals, and animals, as shown in Figure 2.5.

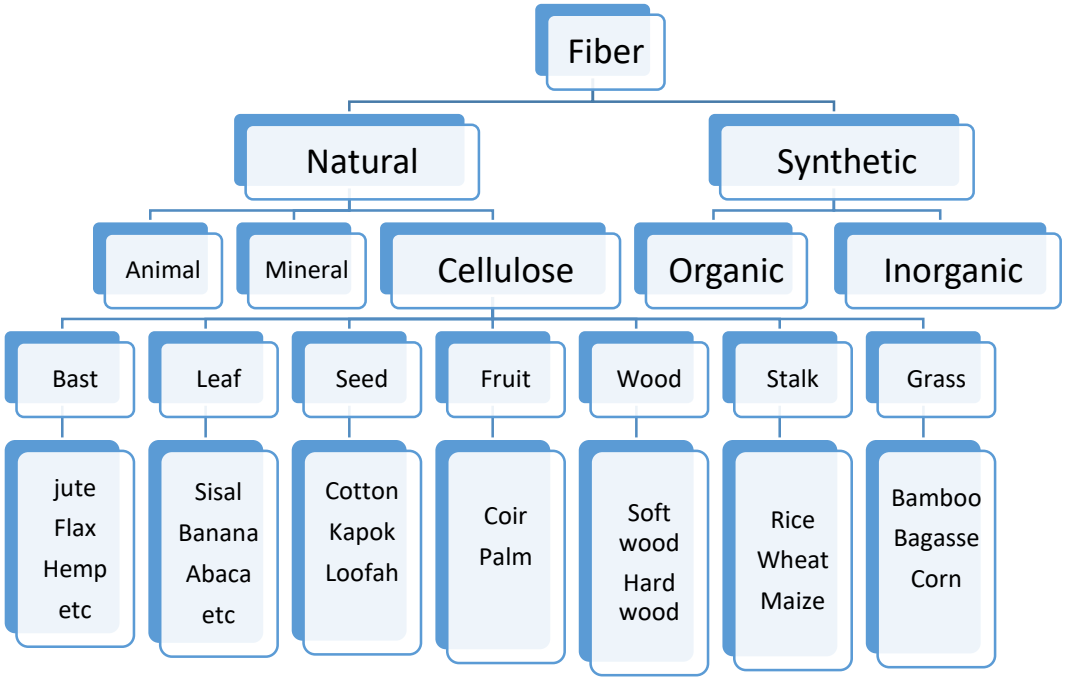

Figure 2.3: Classification of FRP composite fibers [18]

Plant or vegetable fibers

Plant fibers are the most common source of natural fibers used in composite reinforcement [18]. These natural fibers, also known as lignocellulosic fibers, have recently gained research attention due to a range of impressive advantages they have over their synthetic ones. The physical properties and chemical composition of the embedded natural fibers play a big role in the mechanical properties of natural fiber-reinforced composites [18].

Chemical properties of plant fibers

The chemical composition of plant fibers is dominated by cellulose and lignin atoms. Lignin serves as a glue that holds the fiber cells or cellulose together, influencing the form, structure, and properties of any natural fiber [19]. Whereas the amount of cellulose in a natural fiber determines its mechanical properties, particularly its tensile strength, the nature of the lignin layer determines its chemical reactivity [15]. For Natural fibers, their matrix should be selected carefully. The hydrophilic existence of most composite matrices, which means a strong preference for water absorption, and the hydrophobic consistency of most composite matrices contribute to this. As a consequence of these alternating properties between the fibers and the binders, there is typically a strong propensity for aggregate forming at the interfacial boundary, putting the composite's interfacial bonding at risk [20]. Thermoplastic materials are normally favored over their thermosetting alternatives in the selection of matrices for bio fibers due to their high resilience and properties. Thermosetting plastic matrices are used in up to 30% of NFRCs with plant fiber reinforcement, while thermoplastics are used in the remainder [21]. Polypropylene (PP), polyamide (PA), and polyethylene (PE) are commonly used thermoplastic polymers for this purpose, while phenolic, unsaturated polyester, and resins are commonly utilized thermosetting matrices [22].

Physical properties of plant fibers

Plant fibers have a wide range of physical properties due to their different sizes, shapes, and cell wall thickness. The aspect ratio (also known as the length-to-width ratio) is an important consideration when assessing the mechanical strength of natural fibers. The transverse axis of lignocellulosic fibers has a central hollow cavity known as a "lumen," which reduces the bulk density of the fiber. Although the hollow cavity accounts for the fibers' excellent acoustic and thermal insulation, the density reduction contributes to their low-weight properties. Sapuan et al. weighed 29 samples of natural fibers based on design parameters such as Young Modulus, tensile strength, and density. The study's findings suggested that natural fibers could be used to make automotive dashboard panels [23]. Cheung et al. investigated the mechanical and thermal strengths of natural fibers from animal and plants residues in biomedicals. The study's findings revealed that natural fibers can be used to make biomedical-grade materials [24]. Graupner, Herrman, and Mussig explored the mechanical properties of a variety of renewable fibers in detail. Tensile strength, elongation at break, Young modulus, and Charpy impact tests were the

key assessment criteria for these natural fibers. The study's findings revealed that hemp and kenaf fibers had superior Young modulus and tensile strength values, with cotton having strong impact strength, and lyocell fibers having a combination of high tensile strength, impact strength, and Young modulus [25]. A variety of factors affect the mechanical properties of NFRCs, including fiber weight, processing methods, fiber quality, and the adhesive matrix used [26].

Examples of natural fiber-reinforced composites

Among the many natural fibers available for use in composite reinforcements, the following are some of the most widely used in the manufacturing industries [18]:

i. Sisal fiber-reinforced composites.
ii. Cotton fiber-reinforced composites
iii. Hemp fiber-reinforced composites.
iv. Date-palm fiber-reinforced composites.
v. Coir fiber-reinforced composites.
vi. Flax fiber-reinforced composites.
vii. Hybrid fiber-reinforced composites

Advantages of natural fiber-reinforced composites

Natural fiber-reinforced (NFRP) composites are now used rather than synthetic composites such as glass and fiber reinforced composites, mostly in the automotive industry. This raise is based on the following merits [18]:

(i) Biodegradability, recyclability, and reusability properties, as well as the prospect of thermal recycling, lessen the occurrence of environmental pollution. Lower CO2 emissions and biodegradability make them environmentally friendly.

(ii) Due to their widespread availability and ease of fabrication or machining, they have a lower production cost and less drill wear.

(iii) As compared to E-glass fibers, the modulus-weight ratio is higher, resulting in higher specific stiffness and strength.

(iv) Natural fiber composites do not have any irritation effects on the respiratory and dermal organs.

(v) They are ideal for the automotive industry because of their improved electrical resistance, acoustic balance, and thermal stability. Greater acoustic damping property/noise reduction suitability (reduction).

(vi) Based on applications, carbon and glass fibers with equal volume are much more costly than natural fibers ([11], [18]).

(vii) Natural fibers have a lower density of 1.25 – 1.50 $g\text{cm}^{-3}$ than carbon and glass fibers, which have densities of 1.80 – 2.10 $g\text{cm}^{-3}$ and 2.54 $g\text{cm}^{-3}$, respectively.

(viii) In the case of natural fiber composites, tool degradation, resistance, and wear, which are common in composite machining, are significantly reduced.

(ix) During fabrication, less energy is used.

(x) Due to their exceptional carbon (IV) oxide sequestration capacity, they have little or no impact on global warming ([27], [28], [29]).

Disadvantages of natural fiber-reinforced composites

Natural fibers, on the other hand, have some drawbacks that restrict their mechanical application in some engineering parts. The following are some of the drawbacks [18]:

(i) During the manufacturing process, thermal degradation and fiber breakage occur.

(ii) Non-uniformity of fiber geometry can cause the finished composite to be structurally unstable.

(iii) The weak interfacial adhesion between hydrophilic reinforcing fibers and hydrophilic reinforcing fibers often results in poor composite mechanical properties and fiber swelling [30]. In certain situations, a high rate of moisture absorption occurs, resulting in product failure [31]. This suggests a poor fiber-matrix interface due to poor fiber-matrix adhesion. [32].

(iv) Harvest outcomes have a negative effect on price fluctuations [18]. Furthermore, since it is an agricultural product that is unpredictable and easily influenced by bad weather, there is cost variability by harvest.

(v) The inability to withstand flames.

(vi) If not properly handled, it is prone to pest infestation as well as deterioration from other natural factors such as burning.

(vii) Because of their low degradation temperatures (less than 200^0C), they are only suitable for low-temperature applications [33]. Natural fibers begin to degrade or decompose at temperatures just above 200^0C [11], while carbon fibers begin to degrade or decompose at temperatures greater than 900^0C [34].

In conclusion, natural fiber composites are regarded as environmentally friendly materials that are vital to the production of sustainable goods as a means of properly utilizing the opportunities of natural fiber waste materials while also assisting in their complete disposal.

2.3.1.2 Synthetic fiber-reinforced composites

This is a form of composite material that has synthetic fiber reinforcements. They are often used in applications that need a high strength-to-weight ratio.

The reinforcing fibers in this form of the composite are extracted filaments of traditional materials such as carbon, glass, and basalt, among others. Basalt fiber-reinforced polymer (BFRP), Aramid fiber-reinforced polymer composite (AFRP), Glass fiber-reinforced polymer (GFRP), and carbon fiber-reinforced polymer (CFRP) composites are prominent examples of this composite form widely used in manufacturing [35].

2.3.1.3 Comparison of natural and synthetic fibers

The comparison of the physical and mechanical properties of natural fibers against synthetic fiber is illustrated in Table 2.1.

Table 2. 2: Mechanical properties of synthetic and natural fibers [18].

Fiber	Density (gr/cm3)	Tensile Strength (MPa)	Elastic Modulus (GPa)	Elastic at Break (%)
Jute	1.3	393 - 773	26.5	1.5 – 1.8
Sisal	1.5	511 - 635	9.4 – 22	2.0 – 2.5
Flax	1.5	500 – 1500	27.6	2.7 – 3.2
Hemp	1.47	690	70	2.0 – 4.0

Pineapple	1.56	170 – 1627	60 – 82	2.4
Cotton	1.5 - 1.6	400	5.5 – 12	7.0 – 8.0
Kenaf	1.45	930	53	1.6
E-glass	2.55	3400	71	3.4
Aramid	1.4	3000 – 3150	63 – 67	3.3 – 3.7
Carbon	1.4	4000	230 – 240	1.4 – 1.8

2.4 Hybrid Fiber Reinforced Polymer Composites

The products of fiber-reinforced polymer composites consist of high-strength fibers and modulus embedded in or bonded to a matrix with different interfaces between them. Both fiber and matrix maintain their physical and chemical characteristics in this type. Nevertheless, they create a mixture of characteristics that can not be accomplished by any of the Constituents behaving on their own. In general, the main load-carrying members are fibers, while the surrounding matrix holds them in the desired position, acts as a means of load transfer between them, and protects them from damage to the atmosphere because of high temperatures and humidity [36].

A polymer is classified as a molecule with a long chain that contains, together with strong covalent bonds, one or more repetitive atomic units. A series of several molecules of polymers with a common chemical structure is a polymeric material. In the solid-state, either in a random way, or these molecules are frozen in space in a mixture of random and orderly fashions.

Materials used in the polymeric matrix are [36];

1) Polymer thermo-set (resins).

2) Epoxies are primarily used for applications in aerospace and aircraft.

3) Polyester, vinyl ester: widely used in marine applications and automotive applications

4) Phenolic, used in high-temperature bulk molding materials, polyamides, polybenzimidazole (PBI), polphenolquinoxialine (PPQ), used for aerospace applications.

2.5 Machining of FRC materials

Drilling experiment responses, such as roundness error, thrust force, delamination, surface roughness, wear of the instrument, tool life, depending on parameters of the instrument and process parameters. Parameters of the tool include tool material and geometry, while process parameters include speed, feed rate, and temperature of the spindle. A correlation between the parameters of the tool/method (drilling parameters) and the responses is obtained either analytically or empirically by different researchers. Such experiments are useful in predicting. Before the conduct of the experiment, these studies help determine the responses so that the destruction during drilling can be minimized by appropriately choosing the parameters of the tool/process [62].

Since the method of drilling is one of the most essential processes in the industry, several researchers have been studied to optimize the parameters of machining using Taguchi's Technique to enhance this technique's efficiency [62]. The effect of parameters on machining has been mentioned by few authors and few will be addressed here. Drilling operations on composite laminates are important to have useful results for fastening with other materials [6]. Fiber-reinforced polymer composites are widely used in aerospace, naval and automotive industries, and require defect-free composites.

G.Dinesh et al., performed comparative research on the three types of combination of composite material such as Sisal/cotton, Cotton/Coconut sheath, and Sisal/Coconut sheath reinforced with polyester are fabricated and tested the mechanical properties are tensile, flexural strength, and impact strength using UTM and Izod testing machine respectively. They found that sisal/cotton polyester composite possesses good characteristics when compared to the other two polymer composites [36].

In the optimization of surface finishing and hole diameter accuracy machining parameters in dry drilling processes, **Kurt, et al.,** employed the Taguchi method. Three cutting parameters are designed for minimal surface roughness, such as insertion radius, feed rate, and cutting depth. For process optimization, the rationality of the Taguchi methodology is well known [37].

Davim et al. proposed the methodology using the Taguchi technique and ANOVA to evaluate the relationship between feed rate and cutting speed with delamination in a composite laminate [38].

Korkut et al. also used the Taguchi technique to experimentally assess circularity deviation in the bored hole [39].

A paper entitled 'Evaluation of Thrust Force and Surface Roughness in the Use of Taguchi Analysis and Neural Network Drilling Composite Material' was presented by **C.C. Tsao et al.**. The research covers, an experimental methodology to the assessment of thrust force and surface roughness produced by candlestick drills using regression investigation of tests and RBFN was proposed. The authors find that the drill diameter and feed rate are considered to be the most significant factors that impact the thrust force, while the spindle speed and feed rate are seen to make a high influence on the surface roughness. RBFN is shown to be more powerful than multi-variable regression analysis in confirmation tests to determine drilling brought surface roughness and thrust force in composite material drilling [40].

Surface roughness posed by **Sahoo, P. et al.** affect mechanical properties such as fatigue behavior, corrosion resistance, creep life, etc. Other functional qualities of components such as friction, wear, light reflection, heat transfer, lubrication, electrical conductivity, etc. are also affected [41].

Experimental research on the drilling process of jute fiber reinforced polymer composites was conducted by **Hadi, et al.** This study aimed to evaluate the influence of drill bit types and cutting parameters on thrust force, surface roughness, and delamination size in jute fiber reinforced polymer composites drilling employing an experimental strategy based on the full factorial method. The experimental outcomes showed that the form of drill bit influencing both surface roughness and delamination and is also the most important influencing factor on both defects. HSS twist drill drilling results in a smaller delamination scale than that of Coro-Drill 854 and Coro-Drill 856. It can be due to the HSS twist drill decrease in thrust force and can also be correlated with the soft and non-abrasive quality of jute fiber that makes it suitable for HSS twist drill drilling [42].

The Taguchi Method was developed by **Taguchi et al.** [43] as a statistical method. It was initially designed to improve the quality of manufactured products (development of

manufacturing processes), then its application was applied to many other engineering fields, such as biotechnology, etc. Taguchi's efforts have been recognized by professional statisticians, especially in the creation of models for studying variation. Progress in achieving the desired outcomes requires carefully choosing process parameters and bifurcating them into factors of control and noise. The choice of control factors must be made in such a way that the influence of noise factors is nullified. To achieve the best results of the operation, the Taguchi Method requires the identification of proper control factors. To perform a series of experiments, Orthogonal Arrays (OA) are used. To examine the data and forecast the quality of components to be manufactured, the consequences of these experiments are considered and used [44].

Here, an attempt have been made to demonstrate the application of Taguchi's Method to minimize hole roundness error and surface roughness to boost the surface finish characteristics of drilled hybrid sisal-cotton fiber reinforced polyester composites that will be drilled on the CNC drilling machine. Roundness error and Surface roughness are a measure of the quality of the surface of a product and are factors that have a high impact on the mechanical performance of manufactured products [62].

2.6 Applications of Fiber Reinforced Polymer Composite

The rising need for FRP composites as efficient engineering materials to meet the vast human needs in various areas has boosted many industrial sectors. Due to the depletion of crude oil reserves and the need for a suitable replacement for synthetic(non-renewable) composites, experimental research and the use of FRP composites, particularly natural (renewable) composites, has been needed [45]. The list of application areas is not fully completed since it contains both consumer and industrial applications.

The enormous advancement in technology in recent years has also sparked the need for stronger and more reliable engineering materials. Although it is commendable to improve a design's cost-effectiveness, it is also vital to prioritize the most critical aspects of the design's potential use, such as reliability, eco-friendliness, and re - usability or recyclability [46]. In advanced engineering applications, like those in the aerospace industry, reduced weight materials of high quality including flexural rigidity are required [47]. Although certain traditional materials include a few of these characteristics, their engineering applications have several drawbacks. In

the end, this primarily leads to their replacement. As a result, selecting the right material for an engineering design is a difficult task that necessitates careful consideration [48].

As a result, they are very challenging and useful, based on a detailed understanding of FRP composites' excellent mechanical, thermal, and physical properties. Here are some of the applications of fiber-reinforced polymer composite materials:

- **Automotive:** The application of FRP composites can be divided into three categories. The body, frame, and engine all have components. The first two parts were more well-liked than the third one [11]. The vehicle body is designed to reduce total vehicle weight when making seats, resulting in more energy-efficient vehicles. structural panels and Fuel water tanks for the floor and exterior, spoilers, axle shafts, helmets, gears, bumpers, body panels, and bearings are just a few of the applications for FRP composites [13,14].
- **Aerospace:** This sector used FRP composites for structural applications rather than other sectors in the current period. Through the use of FRP composites, the weight is reduced, resulting in increased speed and payload. The A310 aircraft, designed by Airbus in 1987, made extensive use of composite materials. In the meantime, both aircraft's composite tails were made by Airbus A320 in the same year [11]. FRP composites are used to make aircraft wings, stabilizers, seats, floors, helicopter blades, fuselage, landing gears, fuel tanks, and tail plans, among other things [13]. In addition, truss structures, payload bay doors, manipulator arms, and remote pressure vessels are all built with FRP composites [11].
- **Defense:** Military applications of FRP composites can be traced back to the early Second World War. This was the product of widespread industrial exploitation. Moreover, it encourages the reduction of repair and maintenance costs due to the possibility of improved fatigue and corrosion resistance, and through good fiber design, it allows aircraft flexibility, aero-dynamism, and aero-elasticity, especially in their aerofoil, tails, and wings [11].
- **Marine:** FRP composites could also be used to make warships, ship hulls, and due to their excellent corrosion resistance characteristics. Many such marine vehicles also have the advantage of being smaller, which aids in acceleration (higher cruising speed). In addition, the fuel economy and maneuverability of marine vessels have been improved.

Approximately 90% of all recreational vessels are currently made from composites of glass fiber/polyester or vinyl ester resin [11].

- **Civil infrastructure/building construction:** Because of their reducing weight, corrosion resistance and vibration, and high strength properties, FRP composites are becoming a feasible alternative to concrete and in the construction of buildings and bridges. FRP composites can also be used in the production of floor beams.
- **Domestic:** Desks, chairs, railings, toilet panels, internal and external construction products, and furniture springs are only a few of the household items manufactured from FRP composites [13].
- **Electrical and electronics:** FRP composites are involved in the manufacturing of electrical equipment such as frames, cables, insulators, transformer housing, and other similar products [13].
- **Sports, leisure, and recreation:** This application is focused on the main issues of weight reduction, design flexibility, and vibration absorption. pole-vaulting and Fish caching sticks, bicycle fasteners, swimming panels, sports shoes, baseball bats for archery bows, skis, golf course shafts, tennis and outdoor tennis rackets, surfing, and skate boards all use specialized materials. FRP composite applications in leisure, recreation, and sports are possible due to their versatility in design (FRP composites), vibration damping, and commonly known reducing weight properties [13].
- **Medical Science:** FRP composites are used to make bone plates. These plates are used for implantable devices, fracture fixation, and prosthetics, among other things.

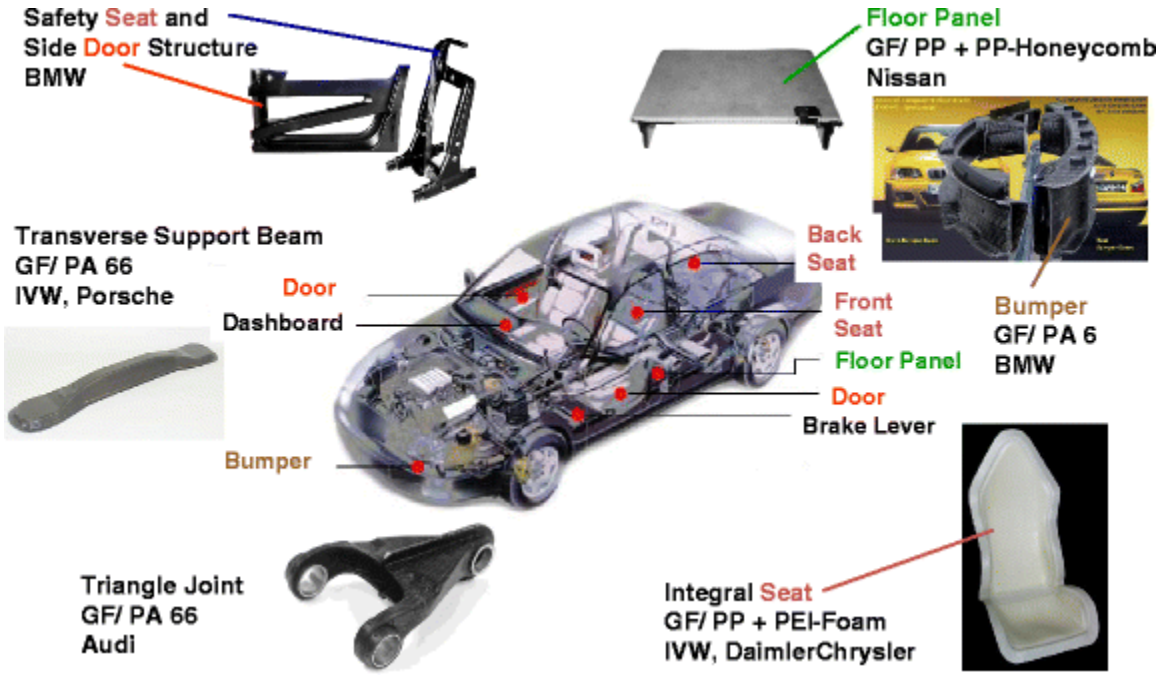

Figure 2.4: Automotive Applications of Composite Materials [49].

2.7 Drilling of Fiber Reinforced Polymer (FRP) Composites

2.7.1 Tooling material selection

Drill tool materials

Drill life is primarily determined by its hardness, thermal resistance, toughness, and wear resistance. A good drill should be able to withstand fracture, wear, and rapid rupture while maintaining hardness at a high temperature. Figures 2.7 and 2.8 demonstrate the main properties of various tool materials.

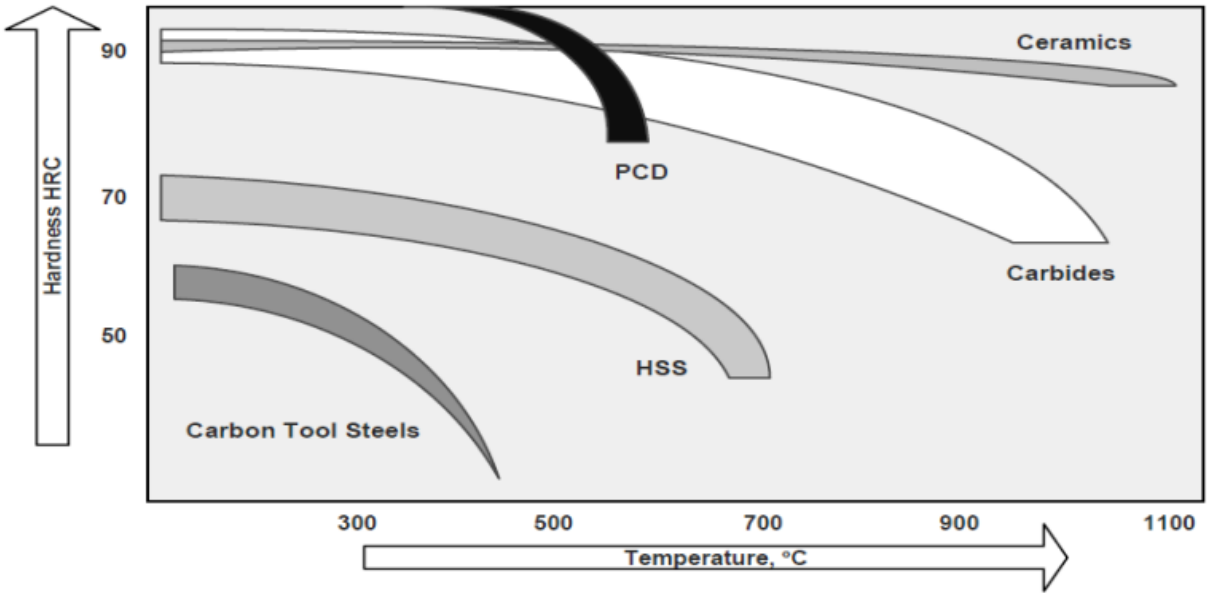

Figure 2.5: Hardness and temperature relationship of drill materials [[50],[51])

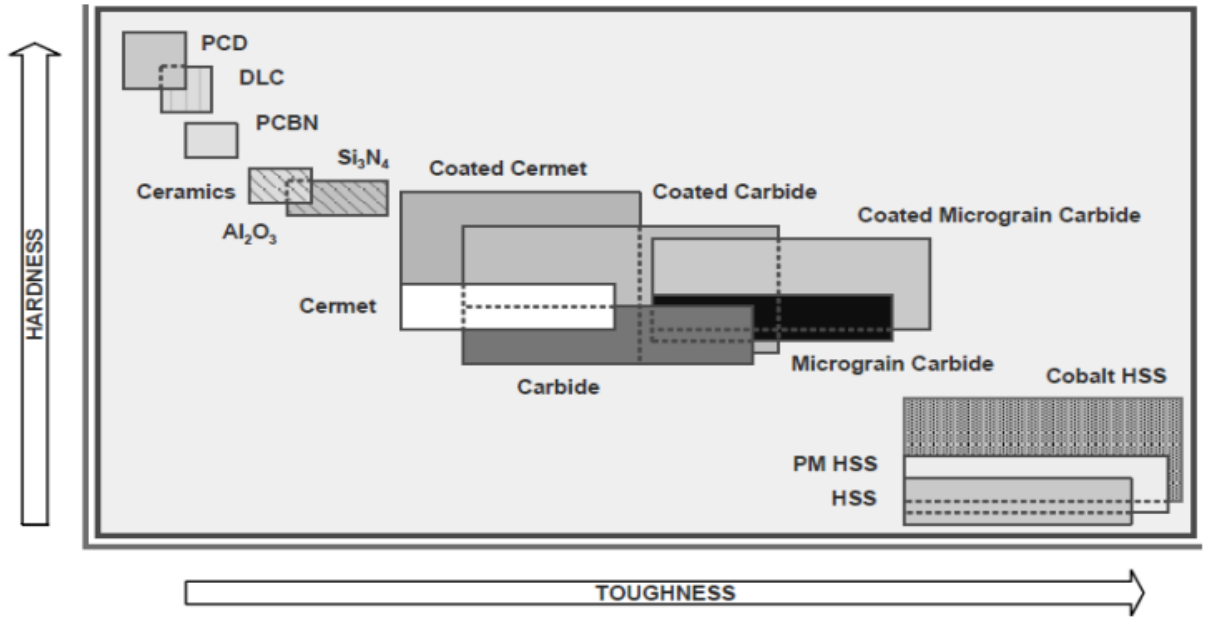

Figure 2.6: Hardness and toughness of drill materials and their relationship ([50], [51]).

As compared to other tooling materials, the toughest tooling material, PCD, has the least property of toughness since its sharp deformation occurs around a temperature of $600\ ^0C$, while HSS has the highest toughness even if it deforms at around$700\ ^0C$.

High-speed steel

Carbide or HSS drill bits have principal attractiveness based on improved output at high cutting speeds compared to other drill bits, according to review analysis of drilling composite laminates [52]. HSS drills were used extensively in some studies ([53], [54], [55]), making it one of the most commonly used tool materials due to its versatility, high durability, and low cost.

Polycrystalline diamond

Garrick claimed to have developed a titanium-stacked veined drill able to drill carbon composites. However, after drilling 200 holes properly, he noticed that wear had developed on the cutting end of the 86 PCD veined drill, which necessitates re-sharpening. Furthermore, it has been stated that it can need improvement with k-lands to improve its cutting edge and enable PCD drills feasible [56]. When compared to other cemented carbide drills, the helical PCD drill geometry had the best overall efficiency, and it was more sensitive to feed rate fluctuation when delamination was taken into account [57].

2.7.3 The drilling operation

Drilling is a machining technique that requires creating or enlarging holes in solid materials. It's a flexible manufacturing process that's essential to any system mating and components. Drilling, which is primarily used as a finishing method, necessitates a high level of accuracy and precision to be successful. The performance of mating between interconnecting parts of any mechanical system is determined in part by the use of the mechanical fasteners including rivets, screws, and pins, among others [62].

Drilling-related machining operations account for about 25% of all machining operations with in manufacturing industry, with an estimated 55,000 drilled holes used to assemble the various parts of the Airbus A350 aircraft [58]. As a result, to achieve successful machine part mating without the use of fasteners, sufficient grooves/holes for their installation must be created, which can only be accomplished through drilling. Mechanical fasteners are expected to create a precise fit into the grooves for that they are designed. They are typically available in numerous standard sizes. As a result, it's important to ensure that riveted or bolted joints are precisely drilled to avoid slackness or unnecessary tightness of fasteners on the machine members. As a

consequence, drilling is a vital machining process that decides whether a machine assembly succeeds or fails [59].

2.8 Gaps in the Research Literature

G.Dinesh et al., performed comparative research on the three types of combination of composite material such as Sisal/cotton, Cotton/Coconut sheath, and Sisal/Coconut sheath reinforced with polyester are fabricated and tested the mechanical properties are tensile, flexural strength, and impact strength using UTM and Izod testing machine respectively. They found that sisal/cotton polyester composite possesses good characteristics when compared to the other two polymer composites [36]. But they didn't study the drilling properties of hybrid sisal-cotton polyester composite even if this composite has good properties compared to other composite materials.

Much research has focused on synthetic or conventional (primarily carbon and glass) fiber-reinforced polymer composites, but little is known about the machinability of natural or sustainable fiber reinforced polymer composites, according to various research works that have been reported under various research literature. Though metal matrix and conventional (mostly carbon and glass) fiber-reinforced polymer composites have been widely machined and optimized their machining parameters in recent years, there is no single study on the machining of natural hybrid sisal-cotton fiber reinforced polyester composite materials.

So this study aims to optimize the machining parameters such as spindle speed, feed rate, and drill diameter to reduce roundness error and surface roughness in drilling natural hybrid sisal-cotton fiber reinforced polyester composite materials.

2.9 Summery

This chapter reviewed the experimental and theoretical concept of composite materials, fiber-reinforced polymer composite, types of fiber-reinforced polymer composite, machining (drilling) of fiber-reinforced composites, applications of fiber-reinforced composite, associated problems of drilling-induced damage on fiber-reinforced composites during the machining process, and the importance of tooling materials and machining parameters (spindle speed and feed rate) in drilling fiber-reinforced polymer composite materials. Furthermore, it explained different kinds

of literature that were performed by Taguchi's method and its effectiveness to implement the optimization of the control variables to the response variables to obtain the favorite responses.

Conclusively, the literature depicts the gaps in the machining of sisal-cotton fiber reinforced polyester composite and drilling parameters (spindle speed, feed rate, and drill diameter) contribute better opportunities for reducing drilling-induced damage, especially roundness error and surface roughness of the composite.

CHAPTER THREE

METHODOLOGY

3.1 Introduction

The materials and experimental methods used in the thesis are discussed in this chapter. This includes matrix and fiber materials, methods of sample preparation, experimental methods and techniques, the process of drilling, and finally, measurement of roundness error and surface roughness of the hybrid sisal-cotton fiber reinforced polyester composite laminate.

The methodology to conduct the overall research is encapsulated shortly in Figure 3.1 below.

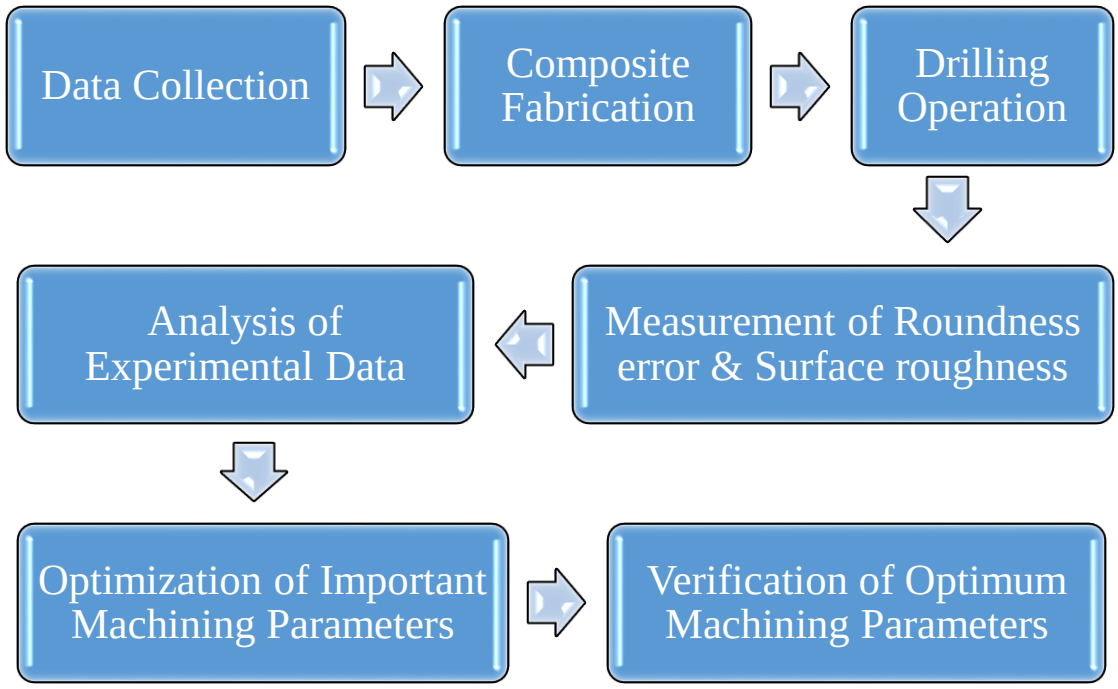

Figure: 3. 1 Methodology

3.2 Materials

3.2.1 Matrix Material-Polyester resin

The fiber materials are bound together by the matrix material and transferred to the fiber material by the applied load on the matrix material and also protected from the atmosphere by the matrix.

Epoxy and polyester are the two most popular resins for thermosets. The polyester resin is inexpensive, durable, and widely used, especially for low-performance purposes, with natural and glass fiber reinforcements. Epoxy resins are more costly than polyester, but in several high-performance applications, their adhesive properties make them useful [8].

The matrix materials used to manufacture HSCFRPC in this research were Polyester resin with catalyst (cobalt), accelerator (Methyl Ethyl Ketone), and releasing agent (polyvinyl Acetate) that are supplied by KADISCO Paint and Adhesive Industry S.C.

3.2.2 Fiber Materials- Sisal and Cotton fiber

Natural fibers which are used as reinforcement are sisal fiber and cotton fiber, and the matrix material is a polyester resin.

For this thesis work, the required amount of sisal plant leaves were collected from Ethiopia, Oromia Region, Dugda wereda, which is located near Meki town. As shown in Figure 3.2 below, the required amount of sisal fiber is extracted from the sisal leaf using a knife. The extracted sisal fiber is put in the sun for five hours after the extraction process to avoid moisture content within the fiber. Finally, the sisal fiber has finished the process of drying and is ready for the next process.

(a) (b) (c) (d)

Figure 3. 2: (a & b). Harvesting sisal plant leaves (c). Extraction Process (d). Extracted sisal Fiber

Following the ES 127 standard, the tensile strength of sisal fiber with sample dimensions of 0.1 mm diameter and 500 mm length and a test speed of 27 mm / min was carried out. The Ethiopian Conformity and Assessment Institute (Ethiopian Standard Agency) conducts a sisal fiber tensile strength test using a universal measuring machine and the results of 15 specimens are taken and encapsulated in the following table and figures. Table 3.1 shows the results of sisal fiber tensile strength, Figure 3.3 shows the experimental setup of sisal fiber on the universal test unit, Figure 3.4 shows the graph of force (N) Vs. time(s) and Figure 3.5 shows stress(N/mm^2) vs. strain (percent) of the sisal fiber during the testing process of tensile strength.

Figure 3. 3: Experimental set up of sisal fiber on the UTM

Test No	Time to Failure (Secs)	Force @ Break (N)	Elong. @ Break (mm)	Elong. @ Peak (mm)	Force @ Peak (N)
1	18.649	10.885	9.337	9.314	11.052
2	19.804	13.288	9.916	9.916	13.288
3	22.384	16.505	11.182	11.182	16.505
4	22.189	13.641	9.252	9.252	13.641
5	22.022	12.553	9.916	9.916	12.553
6	21.844	13.131	9.818	9.818	13.131
7	17.646	6.031	7.932	7.912	6.943
8	19.399	15.004	8.717	8.717	15.004
9	19.881	5.904	8.934	8.915	7.345
10	18.063	5.766	8.115	8.095	7.218
11	18.905	14.063	8.496	8.496	14.063
12	22.114	14.004	9.938	9.938	14.004
13	20.028	14.788	8.995	8.995	14.788
14	19.279	11.336	8.657	8.638	13.465
15	20.014	15.367	8.996	8.996	15.367
Mean	20.148	12.151	9.213	9.207	12.558
S.D.	1.589	3.542	0.839	0.845	3.06
C. of V.	7.888	29.149	9.11	9.173	24.37
L.C.L.	19.268	10.19	8.749	8.739	10.863
U.C.L.	21.028	14.113	9.678	9.674	14.253
Mean - SD	18.559	8.609	8.374	8.362	9.497
Mean + SD	21.737	15.693	10.053	10.051	15.618

Table 3. 1: Sisal fiber tensile strength results

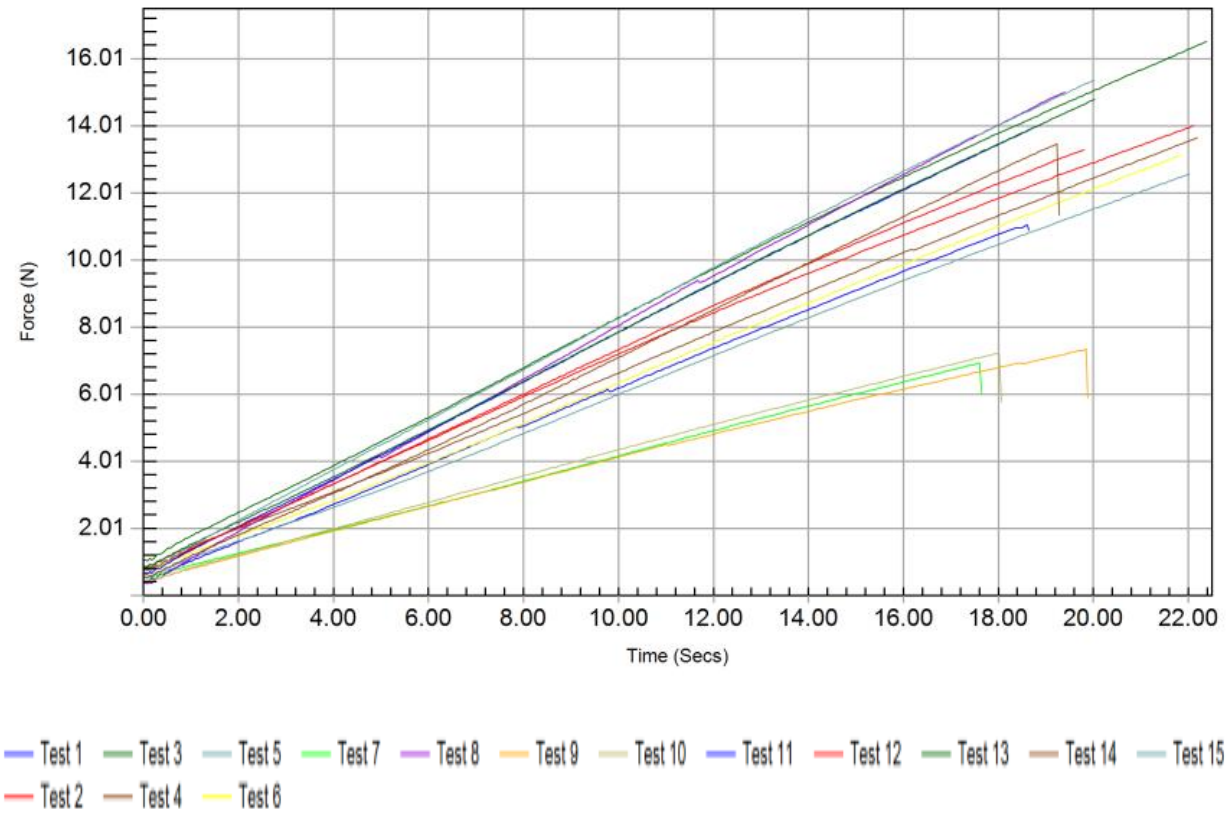

Figure 3. 4: Sisal Fiber Force vs. Time Results

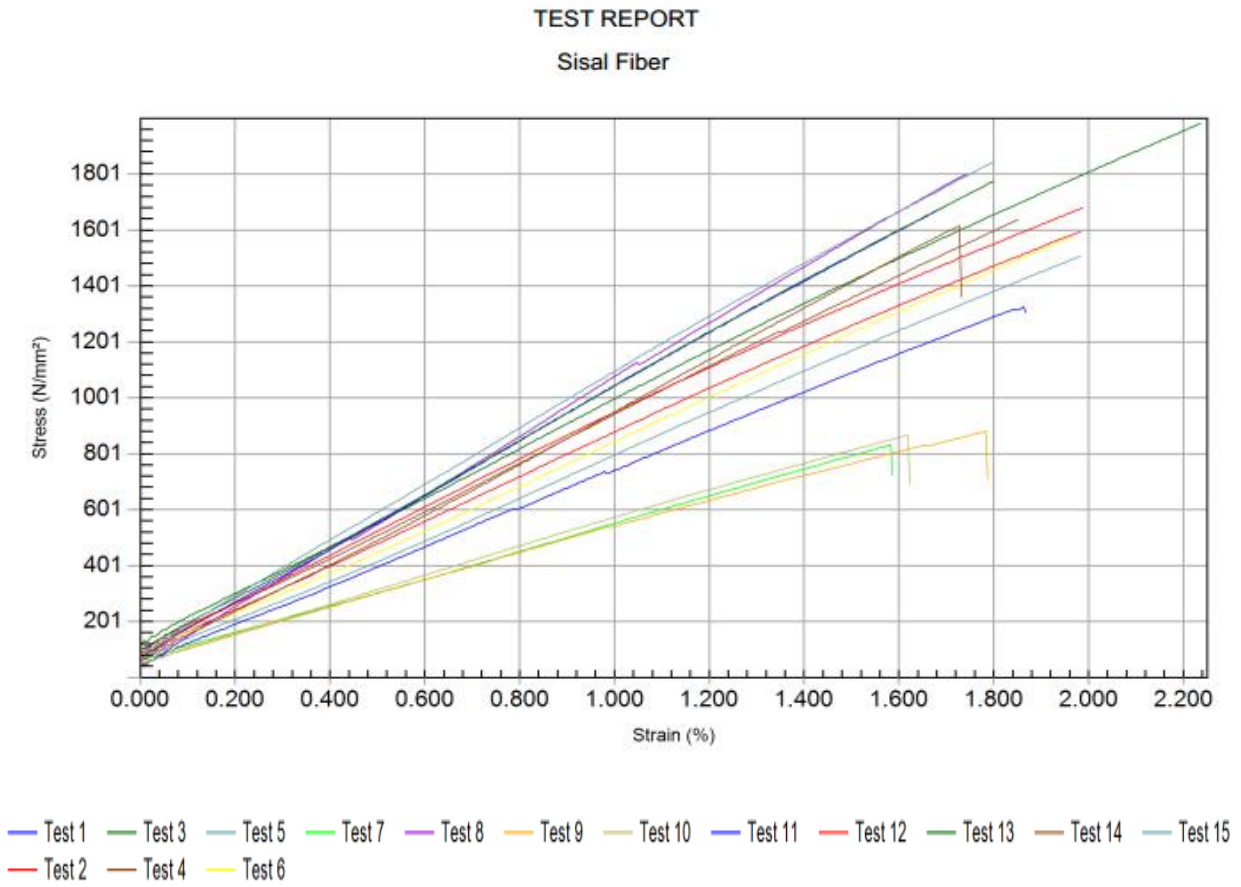

Figure 3. 5: Sisal fiber stress vs strain results during tensile testing

The cotton fibers used in this thesis are obtained from the planting of Awash cotton in the Ethiopia-Oromia region and harvested by Bahir Dar Textile Share company from these cotton seeds. Ginning extracts cotton fiber removed from the seeds, dead leaves, and other debris. It bales the clean cotton again and is ready to be spun. The spun cotton fiber/yarn used in this thesis has a tensile strength of 412 MPa. In figure 3.5, the extracted and processed cotton fiber is shown below in Fig 3.6.

Figure 3. 6: Extracted and processed Cotton fiber/yarn

3.2.3 Materials and Equipment used to Fabricate HSCFRPC

Materials used in HSCFRPC manufacturing are as follows;

- Polyester Resin General Purpose
- Accelerator (Methyl Ethyl Ketone)
- (Cobalt) Catalyst
- Releasing agent (Poly vinyl acetate)
- Stainless steel sheet metal mold
- Hybrid sisal-cotton fiber
- Roller, roller
- Brush
- Flask

3.3 Specimen Preparation Methods

To prepare the sample of the composite material for this thesis, the mass and volume fraction of the fiber and matrix material should be determined first. So, to fabricate the desired composite material specimens, the following calculations were performed.

3.3.1 Mass and Volume Fraction of the Hybrid Fiber and Matrix content of the composite

The hybrid sisal-cotton fiber weight fraction is determined on the foundation of the volume of the matrix. The volume of the matrix is 200 ml and the percent composition of the hybrid fiber is 5 percent cotton and 5 percent sisal (total 10 percent) fiber weight ratio used to create the composite material. The density of the polyester resin is $1.1 g/cm^3$, so the fiber weight is calculated using the following formula.

i. Mass fraction of the fiber and matrix (M_f , M_m)

The total mass of Composite = mass of matrix + mass of fiber

$$M_c = M_m + M_f \quad \text{.....Eq. (3.1)}$$

$$Fiber\ mass\ fraction = \frac{mass\ of\ fiber}{total\ mass}$$

$$M_f = \frac{M_f}{M_m + M_f} \quad \text{.....Eq. (3.2)}$$

$$Matrix\ mass\ fraction = \frac{mass\ of\ matrix}{total\ mass}$$

$$M_m = \frac{M_m}{M_m + M_f} \quad \text{..... Eq. (3.3)}$$

Therefore;

$$M_f + M_c = 1 \quad \text{..... Eq. (3.4)}$$

Calculations;

The hybrid sisal-cotton fiber reinforced polyester composite is prepared from a 10% fiber weight ratio of matrix material content according to the literature [10].

$Mass\ of\ matrix\ material =$ $\boldsymbol{\rho * V = 1.1\ g/cm^3 * 200 cm^3 = 220\ gram}$

$mass\ of\ sisal\ fiber = 5\% * 220 = 11\ gram$

$mass\ of\ cotton\ fiber = 5\% * 220 = 11 gram$

$Total\ mass\ of\ hybrid\ fiber = mass\ of\ cotton\ fiber + mass\ of\ sisal\ fiber$= 11+11

= 22 grams

Therefore;

$\mathrm{M_m} = \frac{\mathrm{M_m}}{\mathrm{M_m}+\mathrm{M_f}} = \frac{220}{242} = 0.9$

$M_f + M_c = 1$

$M_f = 1 - M_c = 1 - 0.9 = 0.1$

$M_f = 0.1$

ii. The volume fraction of the fiber and matrix (V_f, V_f)

$$Volume\ of\ the\ fiber = \frac{mass\ of\ fiber}{density\ of\ the\ fiber}$$

$V_f = \frac{M_f}{\rho_f}$ …….. Eq. (3.5)

$$Volume\ of\ the\ matrix = \frac{mass\ of\ matrix}{density\ of\ the\ matrix}$$

$V_m = \frac{M_m}{\rho_m}$ …….… Eq. (3.6)

$V_c = V_m + V_f$ …….. Eq. (3.7)

$$Fiber\ volume\ fraction = \frac{volume\ of\ fiber}{total\ volume}$$

$V_f = \frac{V_f}{V_F+V_m}$……. Eq. (3.8)

$$Matrix\ volume\ fraction = \frac{volume\ of\ matrix}{total\ volume}$$

$V_m = \frac{V_m}{V_F+V_m}$ …… Eq. (3.9)

Let ρ_f and ρ_m are the density of fiber and matrix respectively. Then we have;

$V_f = \frac{M_f + \rho_m}{M_f\ \rho_m + M_m \rho_f}$ …….. Eq. (3.10)

And;

$V_M = \frac{M_m + \rho_f}{M_f\ \rho_m + M_m \rho_f}$…… Eq. (3.11)

Calculations;

$$Volume\ of\ the\ fiber = \frac{mass\ of\ sisal\ fiber}{density\ of\ sisal\ fiber} + \frac{mass\ of\ cotton\ fiber}{density\ of\ cotton\ fiber}$$

$$V_f = \frac{M_{sf}}{\rho_{sf}} + \frac{M_{cf}}{\rho_{cf}}$$

$$V_f = \frac{11\ gram}{1.3\ gram/cm^3} + \frac{11\ gram}{1.5\ gram/cm^3} = 8.46 + 7.33^{-} = 15.8\ ml$$

$$Volume\ of\ the\ matrix = \frac{mass\ of\ matrix}{density\ of\ the\ matrix}$$

$V_m = \frac{220\ gram}{1.1\ gram/cm^3}$ = 200ml

$Volume\ of\ catalyst\ and\ accelerator = V_{ca} = 2.6\ ml + 2.6\ ml = 5.2\ ml$

$V_c = V_m + V_{ca} + V_f$

$$V_c = 200\ ml + 5.2\ ml + 15.8ml = 221\ ml$$

iii. The density of the composite (ρ_c)

The density of the composite material is determined by its constituents. Constituents of the composites are matrix, fiber and accelerators, and catalysts.

$$\rho_c = \frac{Total\ mass}{Total\ volume}$$

$$= \frac{mass\ of\ matrix}{Total\ volume} + \frac{mass\ of\ catalyst\&accelerator}{Total\ volume} + \frac{mass\ of\ fiber}{Total\ volume}$$

$$\rho_c = \frac{M_m}{V_c} + \frac{M_{ca}}{V_c} + \frac{M_{sf}}{V_c} + \frac{M_{cf}}{V_c} \quad \text{..... Eq. (3.12)}$$

$$\rho_c = \frac{220}{221} + \frac{5.2}{221} + \frac{11}{221} + \frac{11}{221}$$

$$\rho_c = 1.11855 \approx 1.19$$

$$\rho_c = 1.19\ g/cm^3$$

iv. The volume of the mold

The mold volume is prepared to obtain a regular 3 mm ply composite thickness to complete different tests according to their ASTM standards. So, the mold dimension should be 27.15cmx27.15cmx0.3 cm to get 3 mm composite thickness from 221ml volume. The 271.5mmx271.5mmx15 mm stainless steel sheet metal mold is prepared to achieve the desired composite dimension according to this dimension [36].

3.2.2 Preparation of Sisal and Cotton Fiber

The sisal and cotton fiber were chopped into 30 mm lengths using scissors after the extraction process. The weight of 11 grams of cotton and sisal fiber is measured by the automated weight machine ACCULAB GSI-2001, which is available as shown in the figure in the Addis Ababa Tegbare-Id Polytechnic College Biomedical Department Lab. The dimension of the fiber is measured using a tape measure and chopped into 30 mm length as shown in the figure below. In the digital weight machine, the measurement of chopped cotton and sisal fiber is shown below in Fig. 3.7 (a), (b), and (c) respectively.

(a) (b) (c)

Figure 3. 7: (a) Cutting process (b) Cotton fiber weight measurement (c) Sisal fiber weight measurement

3.3.2 Fabrication Procedures

The hybrid sisal-cotton fiber reinforced polyester composite is fabricated by hand lay-up procedure at room temperature. The 271.5 mm X 271.5 mm X 15 mm size rectangular stainless steel mold shown in Fig. 3.8 was used for preparing the composites according to the above calculation to get the necessary dimension. Three specimens are fabricated for this thesis work.

Figure 3. 8: Stainless steel sheet metal Mold

HSCFRPC manufacturing procedures [36];

1. For the preparation of composites, a 271.5 mm X 271.5 mm X 15 mm rectangular mold size is used.
2. In proper proportion, prepare the binding mixture. 2.6 ml of accelerator and 2.6 ml of catalyst are combined for 200ml of GPP resin.
3. Cut the 30 mm long fibers described above.
4. To the mold cavity and top layer, add polyvinyl acetate and allow it to dry.
5. Within the mold, add 100 ml of binding mixture that serves as a matrix of polyester resin.
6. The polyester resin matrix was evenly reinforced by 5 percent of cotton fiber and 5 percent of sisal fiber. The retained fiber weight ratio of 10 percent.
7. Again apply 100 ml of polyester resin until the appropriate size is obtained.
8. Then close the mold and apply 4.07 Mpa pressure using 30 Ton press machine for 5 hours.
9. After drying, we get the two-side smooth flat composite plate.
10. For the other two composite plates, a similar approach was used.

(a)

(b)

(c) (d)

Figure 3. 9: (a & b) Hand Lay-up process (c) HSCFRPC during curing time in the press machine (d) Fabricated HSCFRPC

3.4 Experimental Procedures

3.4.1 Determination of Tensile Strength

A basic material science test is the tensile testing, also known as tension testing in which, in controlled conditions, the material tension loading is carried out on the material. The test results are widely used to choose a composite material for device application, to control consistency, and to foresee how a material would react under other kinds of forces. The properties that are directly measured through a tensile test are ultimate tensile strength, maximum elongation, and decrease in area.

The purpose of the test for this research is to know, check and compare the results of the specimens. Specific to particles or short fiber reinforced plastics, ASTM D3039 is one of the elementary tests used to describe, qualify and verify the tensile characteristics of these products.

For tensile tests, 250 mm x 25 mm x 3 mm dimensions were prepared based on ASTM standard ASTM D-3039. The following Figure 3.10 shows the specimens prepared for tensile tests.

Figure 3. 10: Specimens for tensile test

Tensile tests were performed on the composite specimen prepared with the size of 250mm x 25mm x 3mm by using tensile testing attachments of the universal testing machine in Ethiopian Conformity and Assessment Institute of Ethiopian Standard Agency as shown below in Figure 3.11.

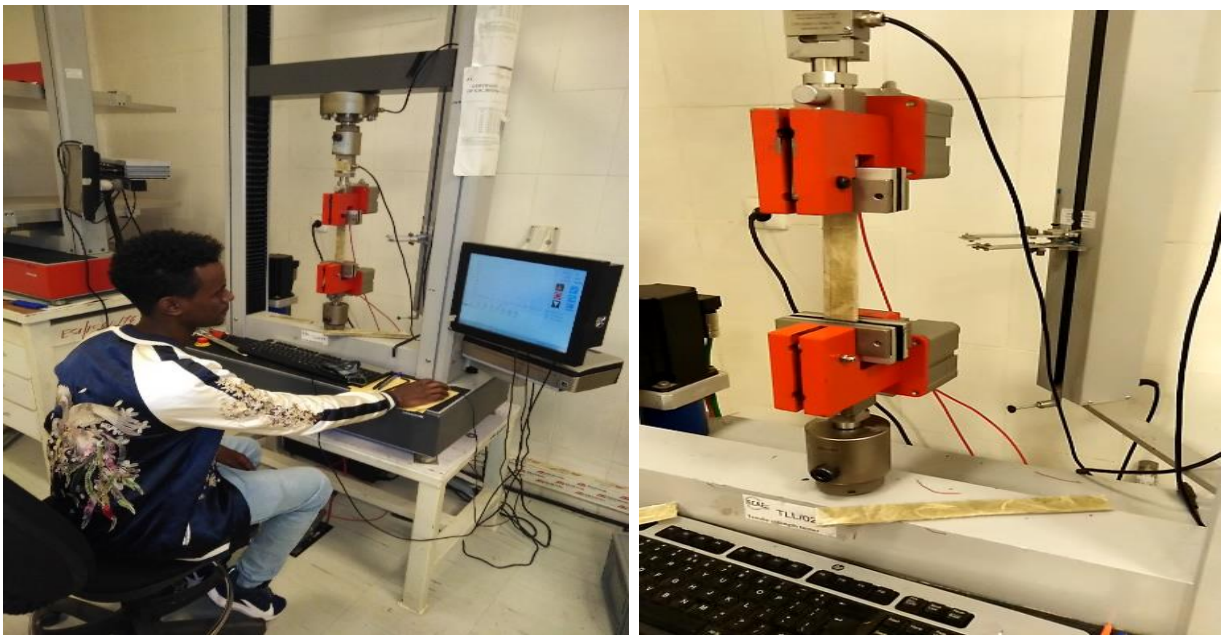

(a) (b)

Figure 3. 11: (a) UTM (M500-100AT) in Ethiopian Standard Agency Lab (b) Specimen under tensile strength testing

As stated in the ASTM, five specimens were prepared with constant rectangular cross-sections. By centering it between the grip interfaces at a defined grip separation, the specimens were put in the grips of a UTM (Model M500-100AT) fixture and pulled until their failure. ASTM D3039 testing was carried out by applying a tensile force to a stressed specimen on a Universal Testing Machine with a typical test speed of 2 mm/min for standard test specimens. To evaluate fundamental tensile properties, an extensometer was used. The universal testing machine measures tensile properties, such as the maximum stress tensile properties applied during the test; peak stress, break stress, break force, peak force, elongation, peak strain, and break strain. On the universal testing machine unit, all these measurements and other method graphical representations are encapsulated in the following Table 3.2, Figure 3.12and 3.13 below.

Test No	Time of Test	Force @ Break (N)	Elong. @ Break (mm)	Strain @ Peak (%)	Strain @ Break (%)	Stress @ Break (N/mm²)	Stress @ Peak (N/mm²)	Force @ Peak (N)
1	29/06 15:27:06	1419.4	2.323	1.658	1.658	18.925	18.925	1419.4
2	29/06 15:29:48	1350.0	2.513	1.793	1.793	18.0	18.0	1350.0
3	29/06 15:34:38	1385.7	2.65	1.889	1.893	18.476	18.513	1388.5
4	29/06 15:56:42	1931.2	3.248	2.32	2.32	25.749	25.749	1931.2
5	29/06 15:58:44	1626.8	3.623	2.586	2.588	21.691	21.793	1634.5
Mean		1542.62	2.871	2.049	2.051	20.568	20.596	1544.72
S.D.		242.379	0.544	0.389	0.389	3.232	3.235	242.617
C. of V.		15.712	18.958	18.974	18.982	15.712	15.706	15.706
L.C.L.		1241.672	2.195	1.567	1.567	16.556	16.58	1243.476
U.C.L.		1843.568	3.547	2.532	2.534	24.581	24.613	1845.964
Mean - SD		1300.241	2.327	1.661	1.661	17.337	17.361	1302.103
Mean + SD		1784.999	3.416	2.438	2.44	23.8	23.831	1787.337

Table 3. 2: Tensile test results

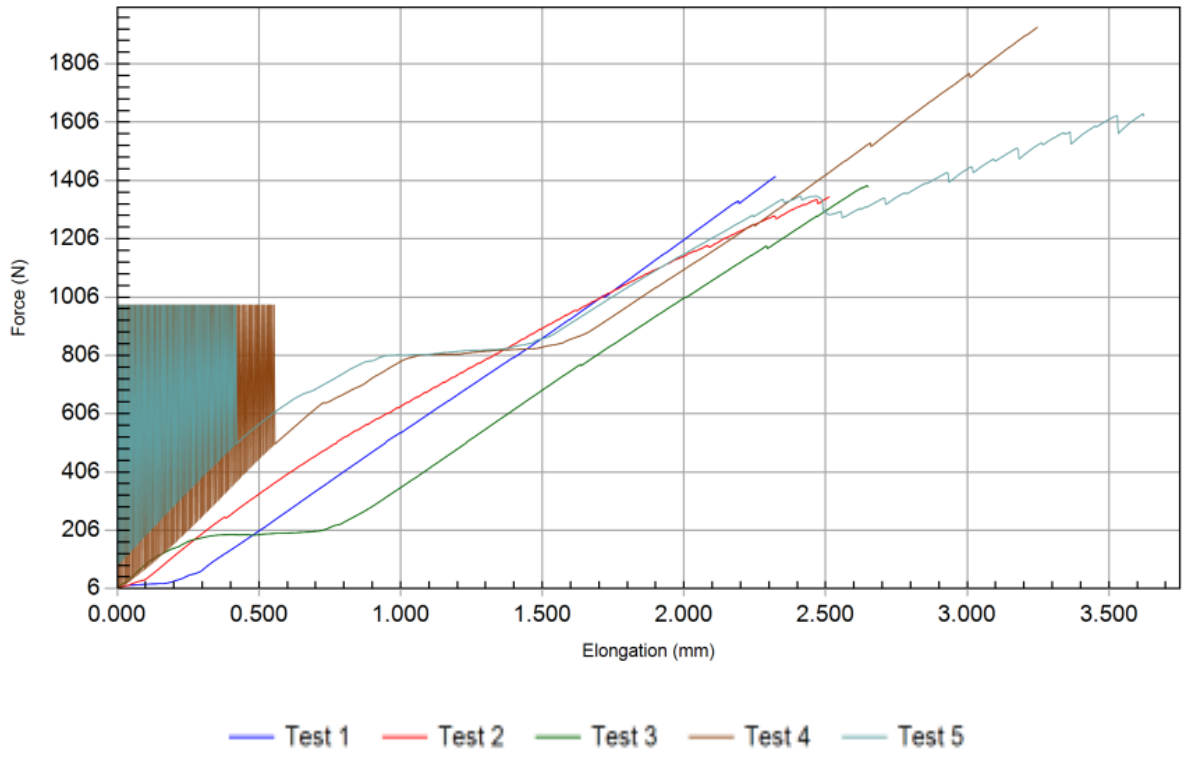

Figure 3. 12: Force vs Elongation Graph

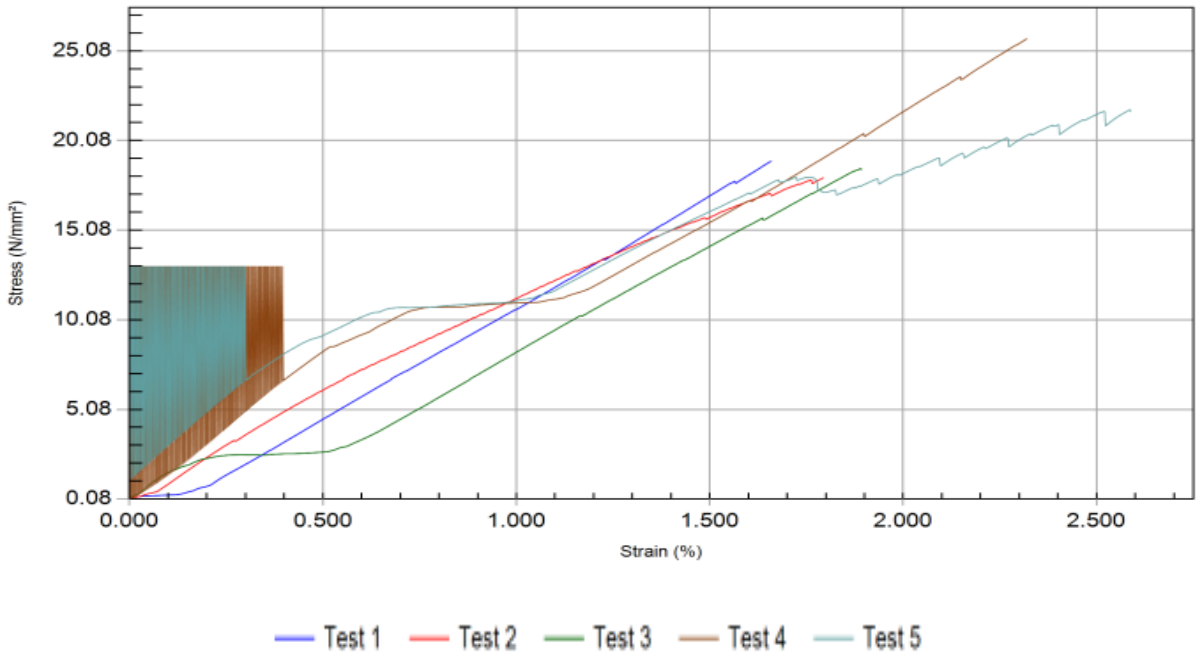

Figure 3. 13: Stress vs Strain Graph

3.4.2 Determination of Impact Strength

The unnotched pendulum impact of the plastic test method as indicated by the energy derived from standardized pendulum-type hammers, placed in standardized instruments, in single pendulum-swing breaking standard specimens, ASTM D4812 covers the determination of plastics' resistance to flexural shock breakage. As absorbed energy per specimen width unit, the result of this ASTM D4812 test method is stated.

The ASTM D4812 test method requires that the failure type be reported as one of the three encoded categories defined as follows for each specimen: C (complete break) A break in which the sample is split into two or more components. P (partial break) is an incomplete break that has broken at least 90% of the specimen's depth. But non-break if the fracture is less than 90% of the specimen's depth in an incomplete break. The purpose of the test for this research is to know, check and compare the results of the specimens.

Following the ASTM D-4812 standard, six specimens were prepared to perform the impact test. As shown in the figure below, each sample was prepared with the size of 64mmx12.7mmx3.2 mm dimensions of ASTM D-4812.

Figure 3. 14: Specimens for impact test

As shown in Figure 3.15 below, impact tests were performed on the digital impact testing machine (model JBS-500B) at Bahir Dar University by ASTM D-4812.

(a) (b)

Figure 3. 15: (a & b) Impact Testing Machine-(JBS 500B) and Experimental Set up

The results of the impact testing machine have been printed and the impact strength is determined by dividing the impact energy in J by the sample thickness. The measuring machine measures and prints out the energy and strength of the effect. The test results and average value of each specimen are encapsulated in the following Table 3.3 below.

Specimen Number	Energy (in joules)	Impact Strength(in KJ/m)
1	53.96	17.98
2	56.46	18.82
3	58.96	19.65
4	51.48	17.16
5	48.23	16.076
6	53.96	17.98
Average	53.8	17.94

Table 3. 3: Impact Testing Results

3.4.3 Drilling Process of HSCFRPC

The impact of three factors with four levels on roundness error and surface roughness were analyzed in this experiment. These factors (control parameters) are the speed of the spindle, feed rate, and drill diameter. In Taguchi's method for three factors and four levels the available orthogonal array matrix is L_{16} orthogonal array. So for this research Taguchi's L_{16} the orthogonal array was selected and correlates spindle speed, feed rate, and drill diameters, which helps to establish an equation for roundness error and roughness of the surface depending on the correlation of these parameters. As shown in the table below, the L-16 Orthogonal array was constructed using Minitab 19 software. The spindle speeds, feed rates, and drill diameters used for drilling operation are summarized below in table 3.4 & 3.5.

Process(control) Parameter	Level 1	Level 2	Level 3	Level 4
A: Spindle Speed (rpm)	600	900	1200	1600
B: Feed Rate (mm/min)	10	15	20	25
C: Drill Diameter (mm)	6	7	8	10

Table 3. 4: Process Parameters and their levels

Experiment number	Spindle Speed	Feed Rate	Drill diameter
1	600	10	6
2	600	15	7
3	600	20	8
4	600	25	10
5	900	10	7
6	900	15	6
7	900	20	10
8	900	25	8
9	1200	10	8
10	1200	15	10
11	1200	20	6
12	1200	25	7
13	1600	10	10

14	1600	15	8
15	1600	20	7
16	1600	25	6

Table 3. 5: L_{16} orthogonal array and the desired parameter values

Composites prepared for this drilling operation have dimensions 228mmx77mmx3mm and the twisted HSS drill bit used for this operation is fabricated by BOSCH Company as shown in Figure 3.16 below. Drill bits used for this thesis work have four different diameters (6mm, 7mm, 8mm, and 10mm) and 135^o point angle.

Figure 3. 16: HSS Bosch Drill Bit

Drilling operation is carried on GSK computer numerical control (CNC) vertical milling machine in Hibret Manufacturing and Machine Building Industry-METEC as shown in the figure below according to Taguchi's design of experiment. The experimental setup of the drilling process is shown below in figure 3.17.

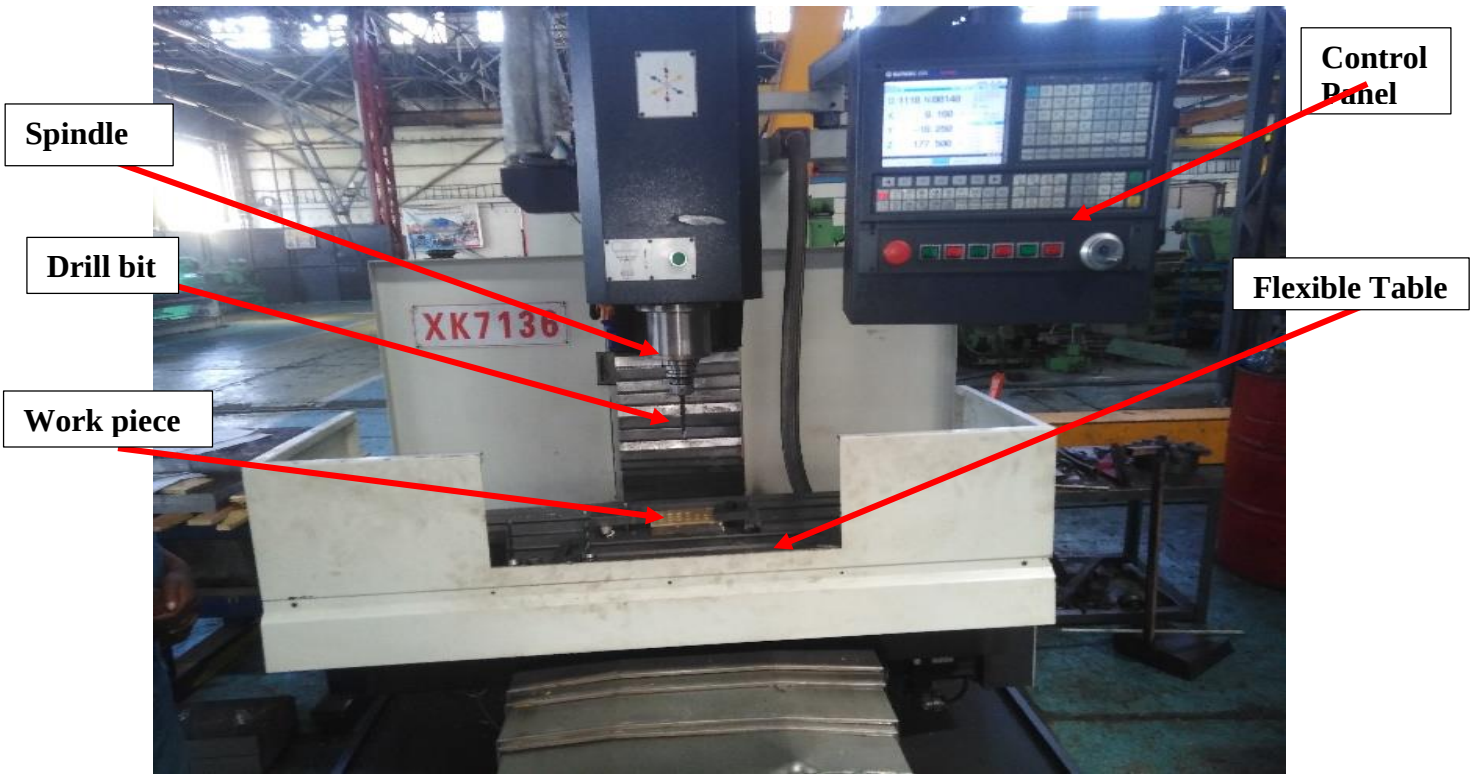

(a)

(b)

Figure 3. 17: (a) CNC Milling Machine and experimental set up (b) Drilling operation

Based on L_{16} orthogonal array part programs are written using Mastercam X4 software for 228mmx77mmx3mm size composite specimen. Four part programs with different spindle speeds, feed rate, and drill diameter are prepared for 16 holes for four drill bit diameters. The first, second, third, and fourth programs were written for 6mm,7mm,8mm, and 10 mm drill bit respectively as listed on APPENDIX D with different spindle speed, feed rate, and drill diameter.

All drilling operations are carried out using the APPENDIX D data. The drawing and the drilled specimen of the hybrid sisal-cotton fiber reinforced polyester composite are sown in figure 3.17 (a) and (b) respectively.

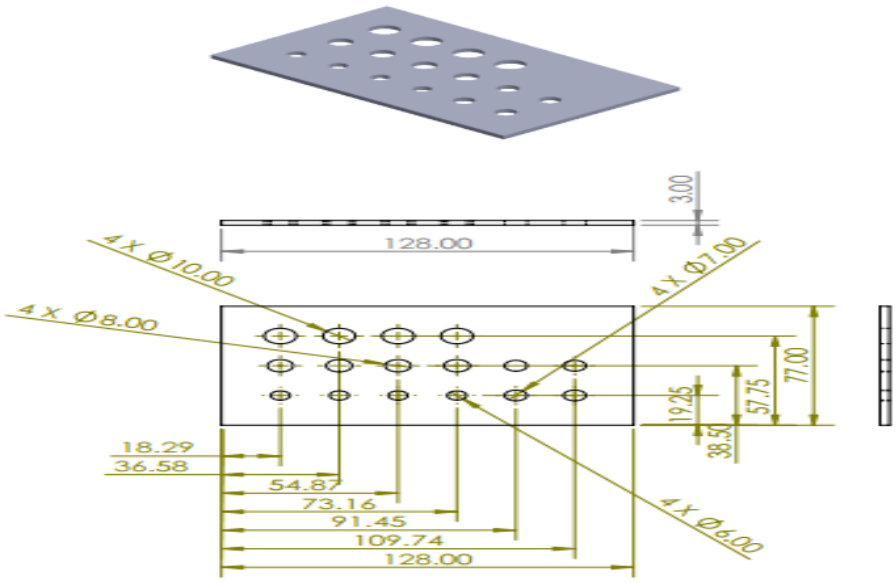

(a)

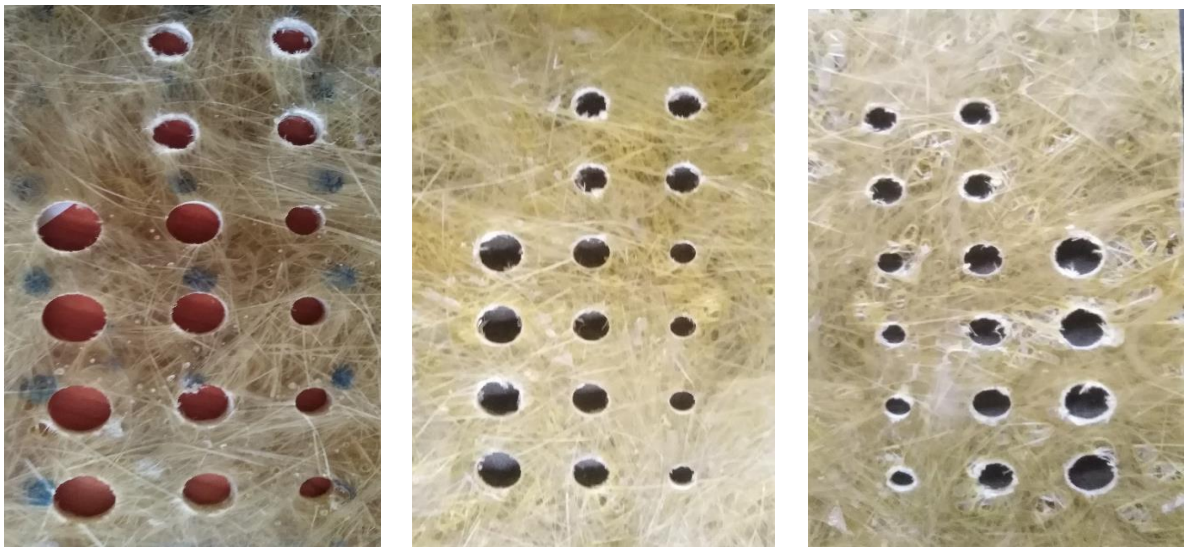

(b)

Figure 3. 18: (a) Specimen drawing (b) Drilled composite Specimen

3.5 Measurement of Roundness Error and Surface Roughness

3.5.1 Roundness Error Measurement

After the drilling operation, the hole qualities in terms of roundness error were measured and analyzed in step by step process. For the circumference of each hole, the minimum and maximum values of diameter are selected out of eight measurements in approximately 22.5-degree difference was taken. The precision HOLEX ABS digital slide caliper having the least count of 0.01 mm was used to measure the variance in diameter of all 16 individual holes of each three composites as shown below in Figure 3.19. The measurement of the internal hole diameter was performed 8 times for each hole using the above-mentioned HOLEX ABS digital caliper. From each measurement, the maximum and minimum values of diameter were entered into the roundness error equation (Eq. 3.13) continuously and the roundness error values were entered into Taguchi's L_{16} orthogonal array for further analysis to get the optimum values to minimize roundness error based on the analysis. Two-point measurement is performed on the outer form by dividing it into four or eight sections. By dividing the difference between the maximum and minimum diameter values by 2, the roundness value is obtained using the following equation [63].

$$\text{Roundness Error} = \frac{D_{max} - D_{min}}{2} \quad \text{..... Eq. (3.13)}$$

(a) (b)

Figure 3. 19: (a) HOLEX digital caliper (b) Measurement of roundness error

After accomplishment of Roundness error measurement inserting the value into L_{16} An orthogonal array table for further analysis and equation development process is performed as shown in Table 3.6 below.

Experiment number	Spindle Speed	Feed Rate	Drill diameter	Roundness Error
1	600	10	6	0.1
2	600	15	7	0.14
3	600	20	8	0.17
4	600	25	10	0.25
5	900	10	7	0.15
6	900	15	6	0.11

7	900	20	10	0.26
8	900	25	8	0.18
9	1200	10	8	0.19
10	1200	15	10	0.26
11	1200	20	6	0.11
12	1200	25	7	0.15
13	1600	10	10	0.28
14	1600	15	8	0.20
15	1600	20	7	0.16
16	1600	25	6	0.12

Table 3. 6: Roundness error Values with different spindle speeds, feed rate, and drill diameter.

3.5.2 Surface Roughness Measurement

To measure surface roughness of drilled sample using zeta 3D optical profilometer first the sample cut into half-section or the diameter cut into a half hole because the light rays are deflected on internal walls of drilled sample to measure their roughness effectively. So the drilled sample cut into half section on the center of diameter and their roughness are measured using 10X lens to get precise and accurate measurement value as shown in the figure above. And the measurement values of surface roughness with different spindle speed, feed rate, and drill diameter are correlated by L_{16} an orthogonal array of Taguchi's matrix and summarized in the following table below.

Experiment number	Spindle Speed (rpm)	Feed Rate (mm/min)	Drill diameter (mm)	Roundness Error(mm)	Surface Roughness (µm)
1	600	10	6	0.1	337.290
2	600	15	7	0.14	324.580
3	600	20	8	0.17	306
4	600	25	10	0.25	309.813
5	900	10	7	0.15	278.810
6	900	15	6	0.11	250.160
7	900	20	10	0.26	270.610
8	900	25	8	0.18	225.156
9	1200	10	8	0.19	230.400
10	1200	15	10	0.26	233.256
11	1200	20	6	0.11	162.480
12	1200	25	7	0.15	155.240
13	1600	10	10	0.28	175.217
14	1600	15	8	0.20	130.746
15	1600	20	7	0.16	98.403
16	1600	25	6	0.12	66.420

Table 3. 7: Surface Roughness and Roundness Error with different spindle speed, feed rate and drill diameter

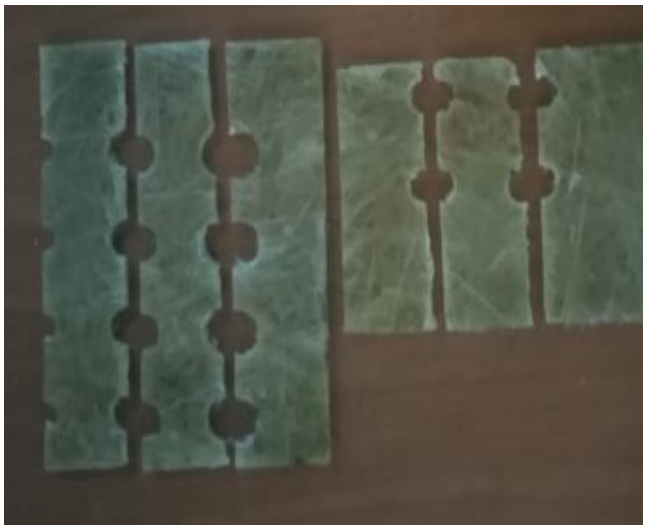

Figure 3. 20: Half Sectioned Samples for Surface Roughness Measurement

The roughness of the surface is measured in a standard unit, usually in microns (μm). The measurement of the surface roughness on the walls of all the drilled holes was performed using Zeta 3D Optical Profilometer (Model: Zeta 20) in Addis Ababa Science and Technology University as shown in the Figure. The experimental setup and its measurement are also depicted in Figure 3.20 below.

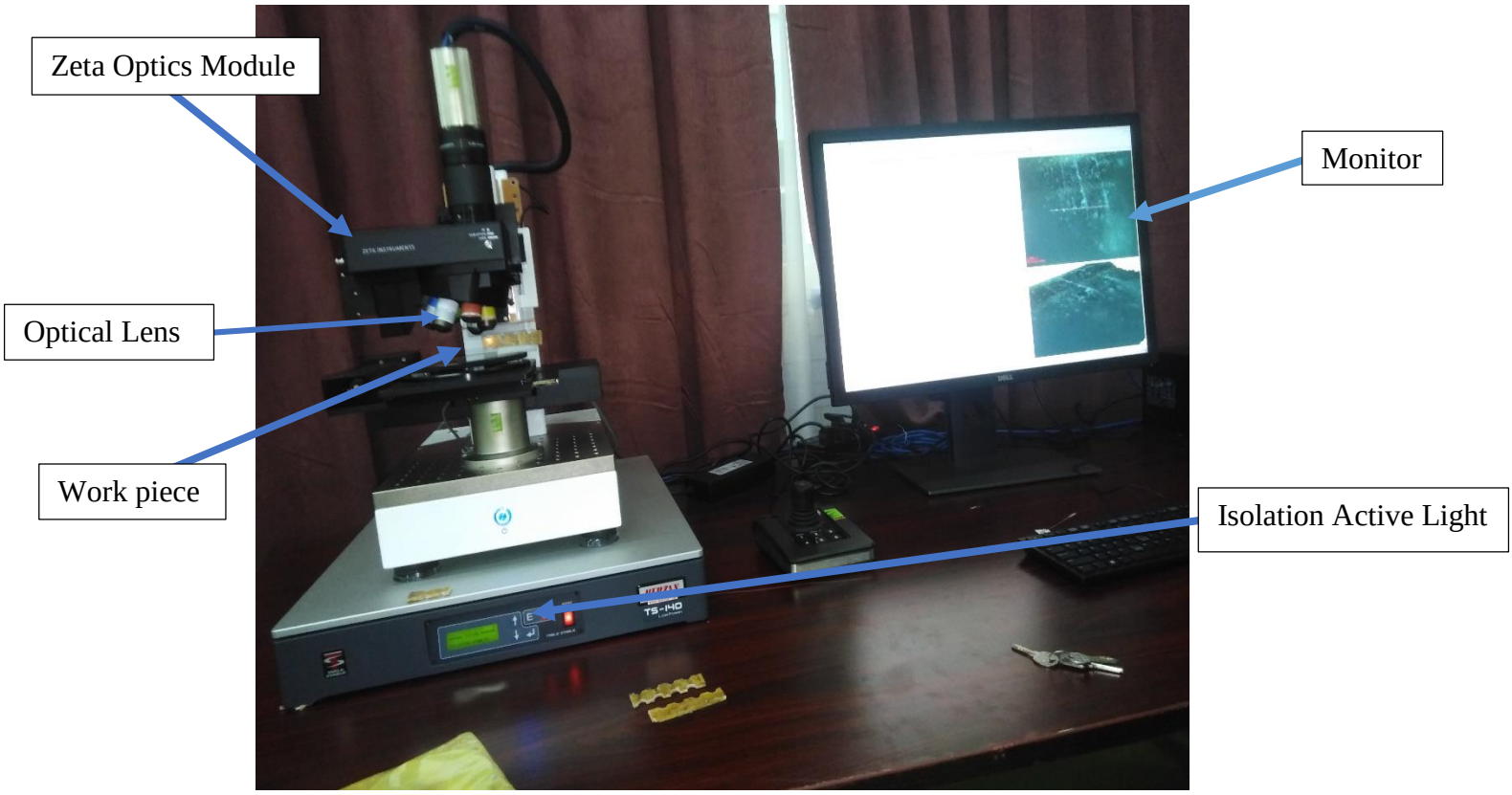

Figure 3. 21: Experimental Set-Up of Zeta 3D Optical Profilometer (Model: Zeta 20)

Zeta 3D optical profilometer measure and display the surface roughness measurements in different parameter units such as Ra, Rq, Rpv, Rp, Rv, Rsk, Rz and Rku. Among these parameters, the selected parameter unit for this study is arithmetic mean roughness (Ra) values for analysis of the surface roughness.

The arithmetic average of the actual values of the roughness feature contours is the Mean Roughness (Roughness Average Ra). In general engineering practice, Ra is one of the most important surface roughness measures widely adopted. It offers a clear general explanation of the variations in surface height. Micrometers, or microinches, are the units of Ra.

Ra means the value generated by the given equations and described in micrometer (μm) when only the reference length of the roughness curve is sampled in the location of the mean line, X-axis in the direction of the mean line, and Y-axis in the path of the longitudinal magnification of this sampled component, and y=f(x) expresses the roughness curve: Ra parameter described and summarized in the following equation.

$$Ra = \frac{1}{l_r}\int_0^{l_r}\{f(x)\}dx \quad \text{..... Eq. (3.15)}$$

Where l_r represents reference length of the roughness.

3.6 Steps of Taguchi's Method

Taguchi Design of Experiment Steps using MINITAB 19

Step 1: In the menu bar select **File > New >Project.**

Step 2: Next, go to the main menu and press the command **Stat > DOE > Taguchi > Create Taguchi Design > Display Available Design.**

Step 3: Select **type of design level, number of factors, available Taguchi designs (with number of factors),** L_{16} then press **Ok** as shown below.

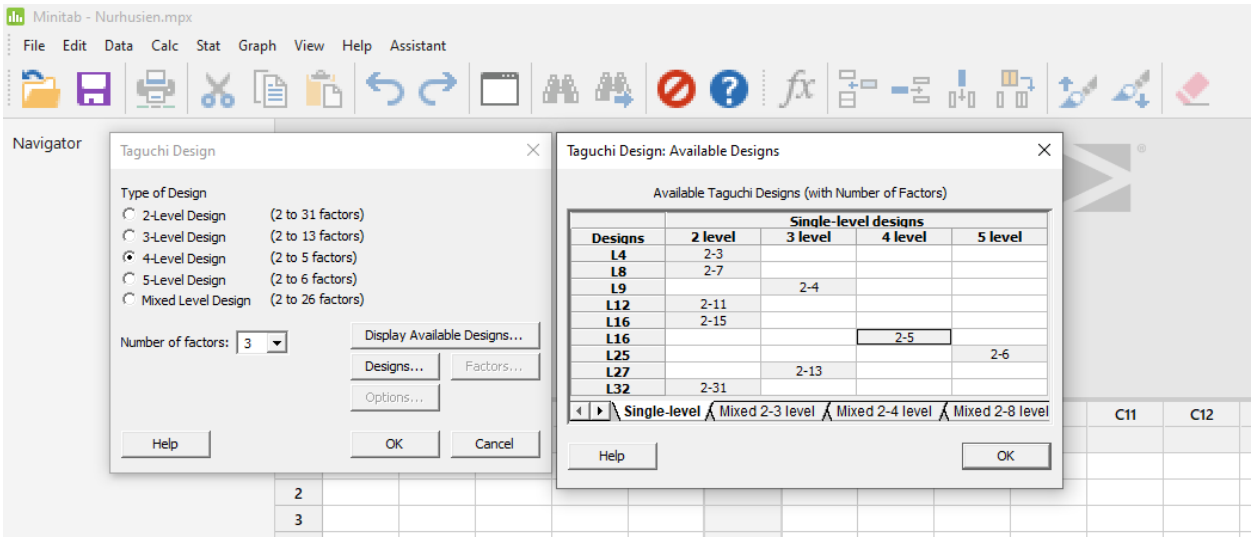

Figure 3. 22: Taguchi Design

Step 4: Enter the **factors name, level values** then press **ok** as shown below.

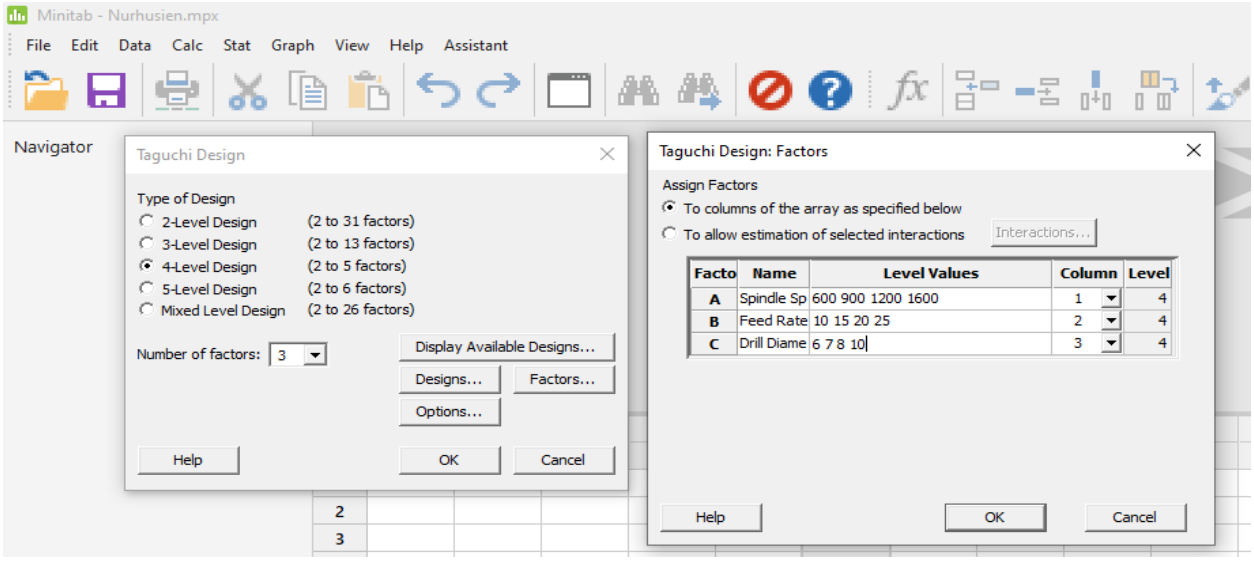

Figure 3. 23: Assigned Design Factors.

Step 5: Finally Taguchi Design Summery window will be displayed as shown below.

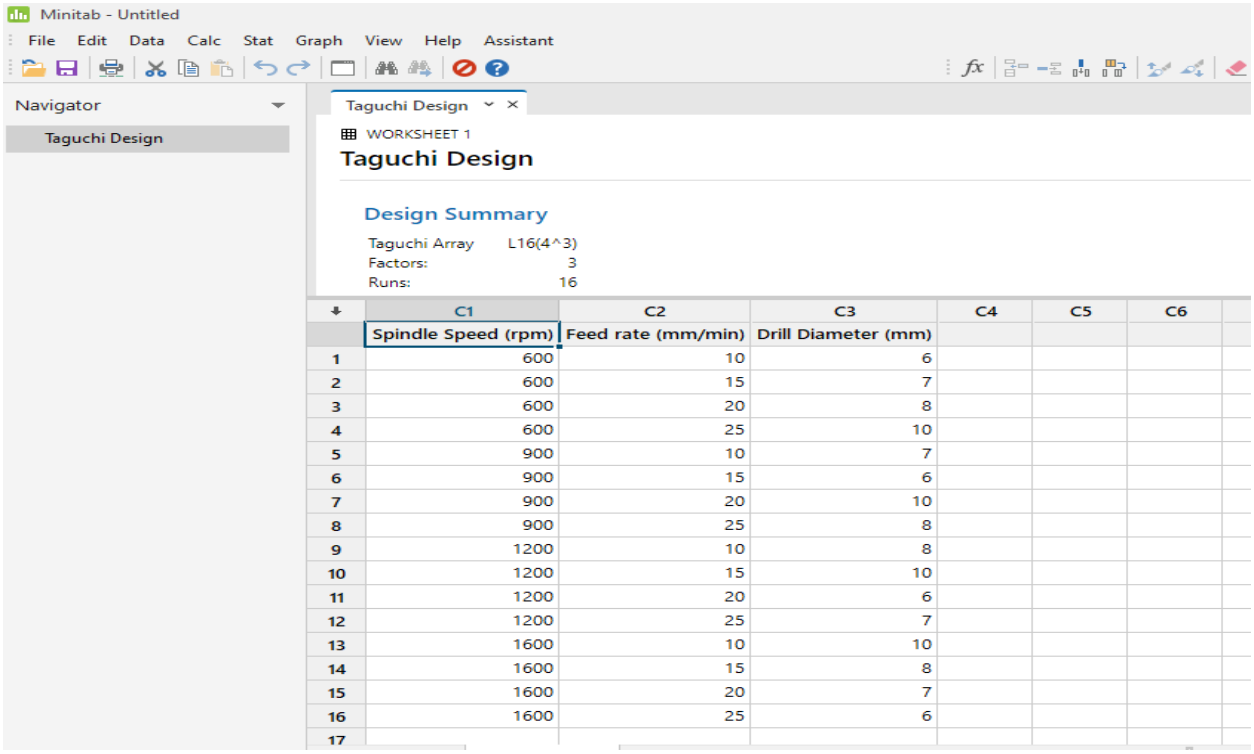

	C1	C2	C3	C4	C5	C6
	Spindle Speed (rpm)	Feed rate (mm/min)	Drill Diameter (mm)			
1	600	10	6			
2	600	15	7			
3	600	20	8			
4	600	25	10			
5	900	10	7			
6	900	15	6			
7	900	20	10			
8	900	25	8			
9	1200	10	8			
10	1200	15	10			
11	1200	20	6			
12	1200	25	7			
13	1600	10	10			
14	1600	15	8			
15	1600	20	7			
16	1600	25	6			
17						

Figure 3. 24: Taguchi Design Summery

Steps of Regression Analysis Using MINITAB 19 Software

After filling experimental roundness error results into the Taguchi design summary table the subsequent stages have been done to develop a roundness error equation in terms of spindle speed, feed rate, and drill diameter.

Step 1: In the menu bar select the command **Stat > Regression > Regression > Fit Regression Model**

Step 2: Enter the **Responses** and **Continuous predictors of regression** as shown below.

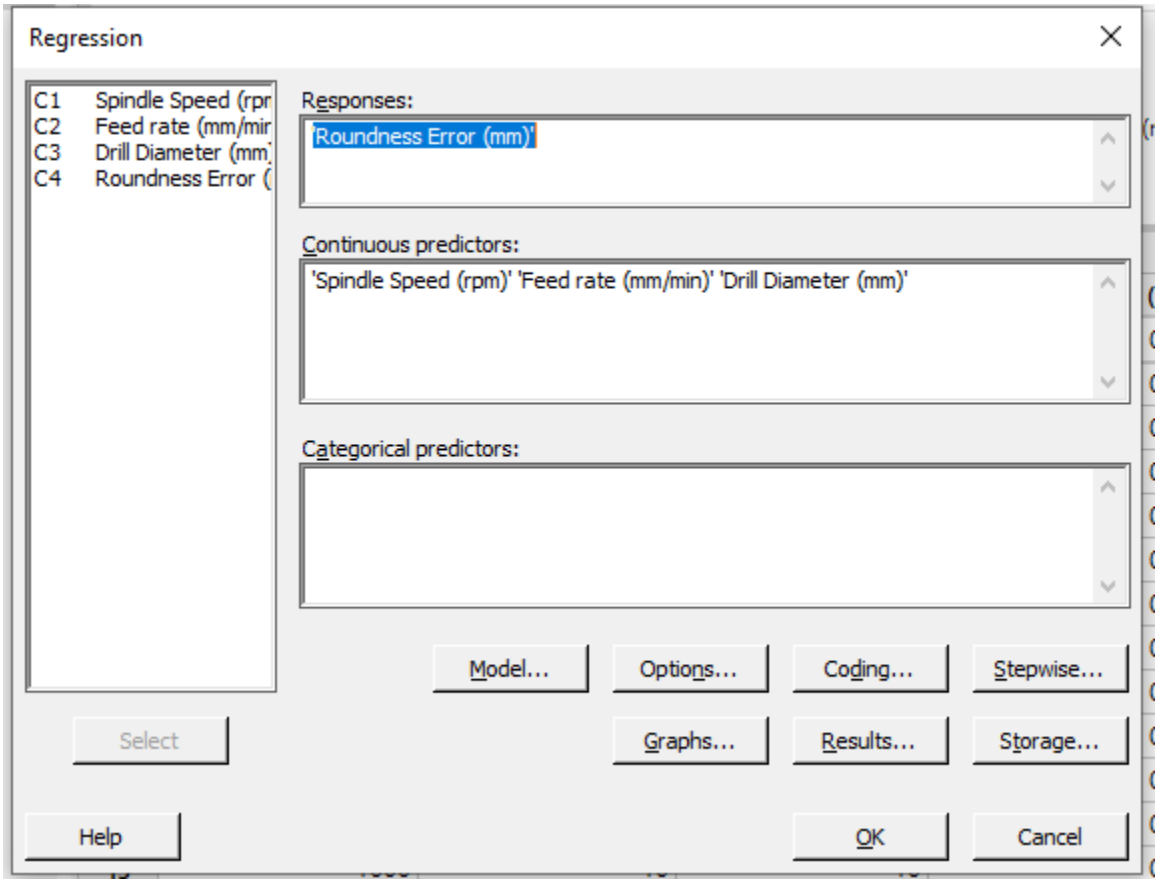

Figure 3. 25: Responses and Continuous Predictors of the regression

Step 3: Finally Press **OK** and Regression Equation for Roundness Error will be displayed.

Steps of Signal to Noise Ratio Analysis using MINITAB 19 Software

Step 1: In the menu bar select **Stat > DOE > Taguchi > Analyze Taguchi Design**

Step 2: Select **roundness error in the response data** and then **Signal to Noise Ratio predictors** as shown below.

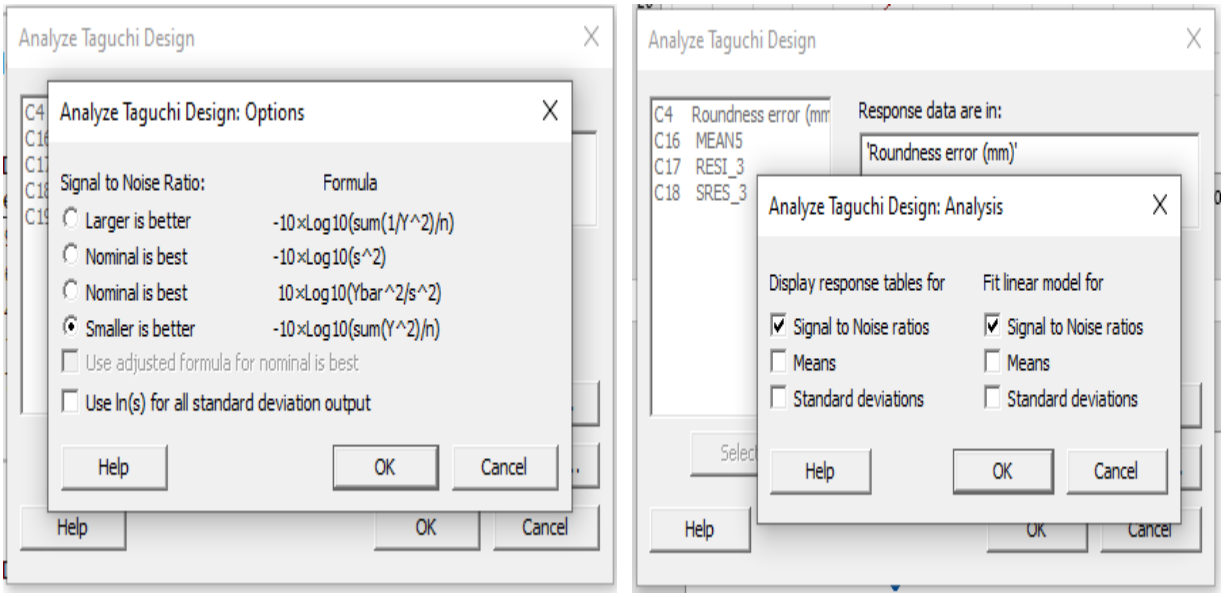

Figure 3. 26: Signal to Noise Ratio Predictors and Responses.

Step 3: Finally Press OK and Signal to Noise Ratio responses for Roundness Error will be displayed.

Steps of ANOVA using MINITAB 19 software

Step 1: From the MINITAB 19 menu bar select the command**:**

Stat > ANOVA > General Linear Model > Fit General Linear Model.

Step 2: Select the response and factors of the General Linear Model in the window appeared by step 1 commands.

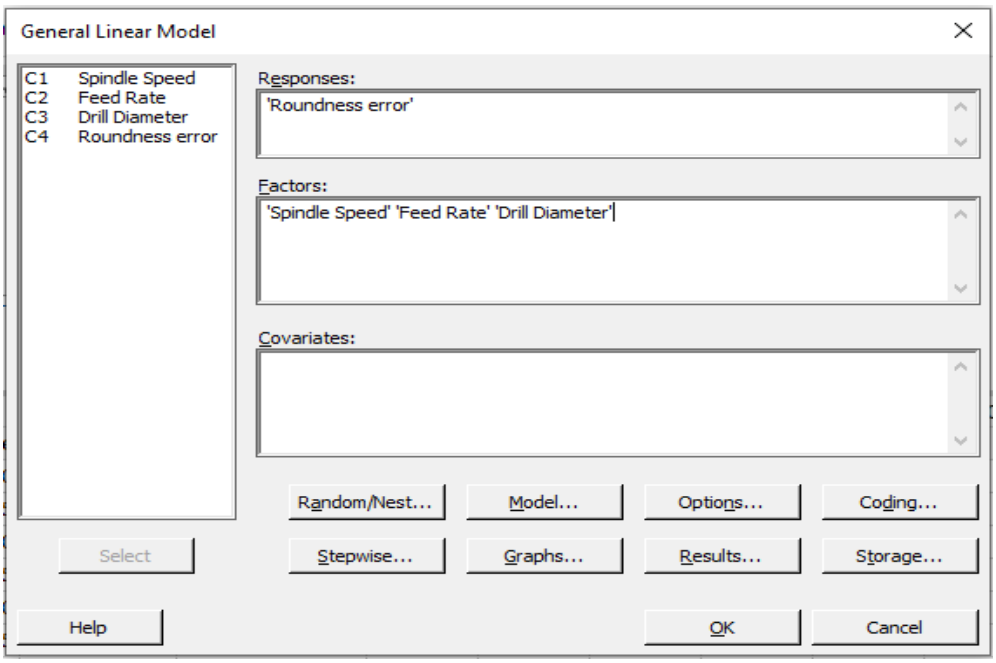

Figure 3. 27: General Linear Model

Step 3: Press **OK** and analysis of variance will appear in the table will be shown.

CHAPTER FOUR

RESULTS AND DISCUSSIONS

4.1 Introduction

This chapter includes the results and discussions on roundness error and surface roughness using Taguchi's method. The three drilling parameters (spindle speed, feed rate, and drill diameter) were correlated with the responses of the roundness error and surface roughness using Taguchi methods after conducting the drilling procedure and measurement of roundness error and surface roughness. Using the commercial software package MINITAB 19, a series of experimental results based on the L_{16} the orthogonal array was obtained and analyzed. To relate the selected drilling parameters to the quality characteristics of the drilled holes, linear regression equations have been established. To determine the impact on the quality of drilled holes of the drilling parameters, Taguchi orthogonal arrays were used, as well as signal to noise (S/N) ratio, variance analysis (ANOVA), and regression analysis.

4.2 Results and Discussions on Roundness Error

4.2.1 Regression Analysis

The purpose of regression analysis is to correlate the control parameters and response parameters using an equation or formula based on the experimental data. In designing the mathematical model for roundness error, the cutting speed, drill diameter, and feed rate are taken into account. For drilling conditions on hybrid sisal-cotton fiber reinforced polyester composite, the correlation between the considered drilled parameters and roundness error is obtained by linear regression process. Based on roundness error measurement results, the linear polynomial model equation is generated using commercially available MINITAB 19 software for different drilling parameters and written below in Eq. 4.1.

Regression Equation

$$R_E = -0.14180 + 0.000028\,S - 0.000495\,F + 0.038493\,D \quad \text{..... Eq. (4.1)}$$

Where, R_E is roundness error in mm, S is spindle speed in rpm, F is feed rate mm/min and D is drill diameter.

Based on the above equation the Predicted values for roundness error have been summarized in the following table and compared to the experimental result in their percentage error (deviation from the experimental result).

Trials	Experimental values	Predicted values	Predicted value error in %
1	0.10	0.101	1
2	0.14	0.137	2.14
3	0.17	0.174	2.35
4	0.25	0.247	1.2
5	0.15	0.147	2
6	0.11	0.1069	3.1
7	0.26	0.25843	0.604
8	0.18	0.1789	0.61
9	0.19	0.1948	2.53
10	0.26	0.2693	3.58
11	0.11	0.113	2.72
12	0.15	0.1489	0.73
13	0.28	0.283	1.07
14	0.20	0.2035	1.75
15	0.16	0.1626	1.625
16	0.12	0.122	1.66

Table 4. 1: Experimental and Predicted Values of Roundness Error

The experimental and predicted values are shown in Table 4.1. And also the estimated values are compared to experimental values using a comparison graph and shown below in Fig. 4.1.

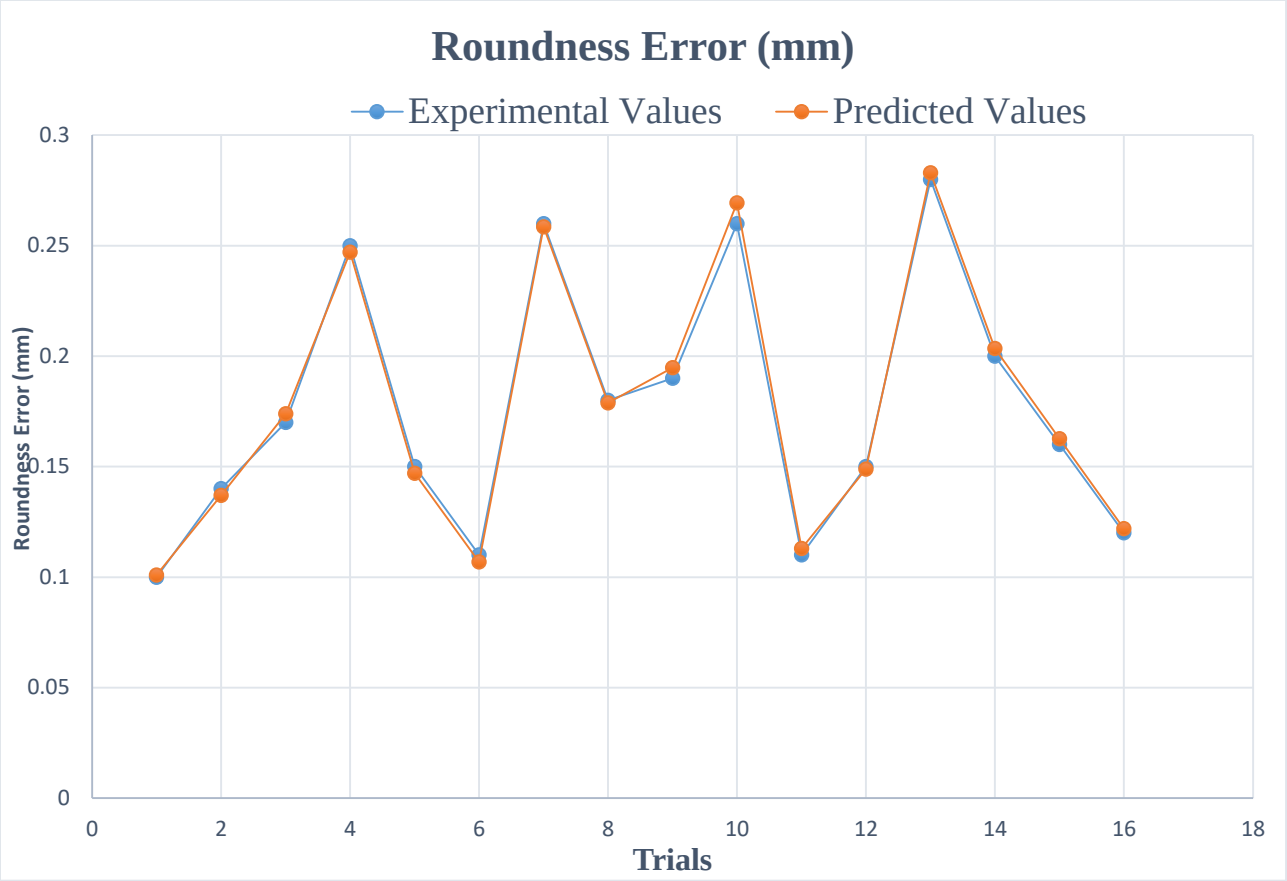

Figure 4. 1: Comparison of Experimental and Predicted Values of Roundness Error.

4.2.2 The Signal to Noise Ratio Analysis

In the Taguchi process, the term signal is the desirable value (mean) for the output characteristic and the term noise is the undesired value (deviation, SD) for the output characteristic. The S / N ratio, therefore, is the average to SD ratio. To evaluate the quality attribute that deviates from the target value, Taguchi uses the S / N ratio. Depending on the type of characteristic, there are several S / N ratios available; lower the better, nominal the best, and higher the better [60,61].

Smaller the better:

$$S/N_L = -10\log\left(\frac{1}{n}\sum_{i=1}^{n} y_i^2\right) \quad \text{Eq. (4.2)}$$

Where y is the observed data, and n is the number of observations.

So the effect of the above parameters on roundness error is evaluated based on the roundness error result.

Experiment number	Spindle Speed (rpm)	Feed Rate (mm/min)	Drill diameter (mm)	Roundness Error(mm)
1	600	10	6	0.1
2	600	15	7	0.14
3	600	20	8	0.17
4	600	25	10	0.25
5	900	10	7	0.15
6	900	15	6	0.11
7	900	20	10	0.26
8	900	25	8	0.18
9	1200	10	8	0.19
10	1200	15	10	0.26
11	1200	20	6	0.11
12	1200	25	7	0.15
13	1600	10	10	0.28
14	1600	15	8	0.20
15	1600	20	7	0.16
16	1600	25	6	0.12

Table 4. 2: L_{16} orthogonal array of spindle speed, feed rate, drill diameter, and roundness error

Using the data presented above with the formula chosen above to measure S / N ratio, the results of the Taguchi experiment are summarized in Table 4.2 above and presented below in Fig. 4.2, which was obtained using the statistical software MINITAB 19. From the S / N responses, it can

be noted that drill diameter is the most significant factor influencing roundness error since, as shown in Table 4.3 below, it is put in the first rank relative to other parameters.

Response Table for Signal to Noise Ratios

Smaller is better

Level	Spindle Speed	Feed Rate	Drill Diameter
1	16.21	15.35	19.05
2	15.59	15.56	16.65
3	15.27	15.43	14.58
4	14.75	15.48	11.54
Delta	1.46	0.21	7.51
Rank	2	3	1

Table 4. 3: Response table for the signal to noise ratios

Fig. 4.2 shows the effect of drilling parameters on hole diameter error and the optimum values based on their rank. According to the analysis and the main effect plot graph for SN ratios the optimum values to minimize roundness error are; 600rpm, 15 mm/min, 6mm of spindle speed, feed rate, and drill diameter respectively.

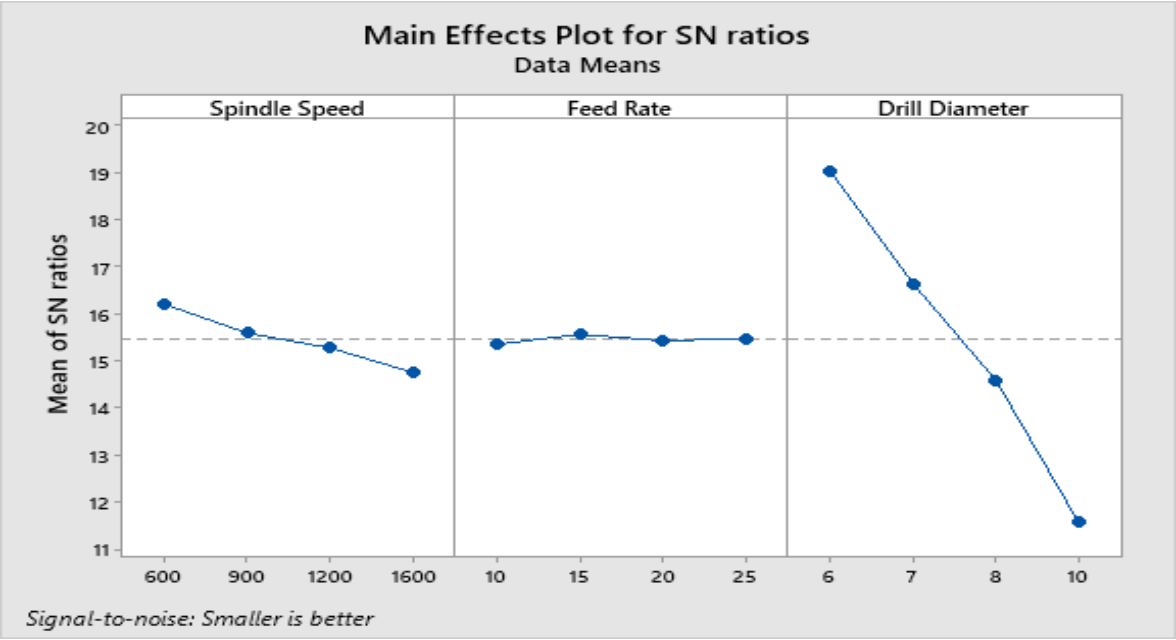

Figure 4.2: Main effect plot for means of SN ratios of roundness error

4.2.3 Analysis of variance

A variance analysis (ANOVA) determines the relative significance of the factors concerning their percentage contribution to the reaction [60, 61]. For the valuation of the variance of error for the special effects and the confidence interval of the prediction of the error, ANOVA is also required. To acquire the percentage contribution of each of the parameters, the analysis was performed based on their S / N ratios.

DF: Degree of freedom, SS: Sum of squares, Contribution: percentage contribution, Adj SS: adjusted sum of squares, Adj MS: adjusted mean of squares, F-value: variance, P-value: calculated probability with a confidence interval of 95 percent is displayed as follows:

Analysis of Variance

Source	DF	Seq SS	Contribution	Adj SS	Adj MS	F-Value	P-Value
Spindle Speed	3	0.001716	3.19%	0.001716	0.000572	102.81	0.000
Feed Rate	3	0.000137	0.25%	0.000137	0.000046	8.19	0.015
Drill Diameter	3	0.051877	96.49%	0.051877	0.017292	3108.72	0.000
Error	6	0.000033	0.06%	0.000033	0.000006		
Total	15	0.053762	100.00%				

Table 4. 4: ANOVA for response

From Table 4.4, observation can be made such that the drill tool diameter (96.49 percent) has a greater impact on roundness error and feed rate, spindle speed accounts for 3.19 percent and 0.25 percent contribution respectively on roundness error.

4.3 Result and Discussion on Surface Roughness

The three drilling parameters (spindle speed, feed rate, and drill diameter) were correlated with the responses of the surface roughness using Taguchi methods after conducting the drilling procedure and measuring the surface roughness of the HSCFRPC samples. Using the

commercial software package MINITAB 19, a series of experimental results based on the L_{16} the orthogonal array was obtained and analyzed. To create a connection between the selected drilling parameters and surface roughness characteristics of the drilled holes, linear regression equations have been established. To estimate the influence of drilling parameters on the feature of drilled holes, Taguchi orthogonal arrays, the signal to noise (S / N) ratio, the analysis of variance (ANOVA), and regression analysis were used and interpreted in the following analysis.

4.3.1 Regression Analysis

In designing the mathematical model for surface roughness of the drilled hole, the cutting speed, feed rate, and drill tool diameter are taken into account. For drilling conditions on hybrid sisal-cotton fiber reinforced polyester composite, the correlation between the surface roughness and drilling parameters of the holes considered and the guiding equation is obtained by linear regression. Based on surface roughness measurement results, the linear polynomial model equation is generated using commercially available MINITAB 19 software for different drilling parameters and written below in Eq. 4.3.

Regression Equation

$$S_R = 434.38 - 0.20213\ S - 4.482\ F + 10.779\ D \quad \text{Eq. (4.3)}$$

Where, S_R is surface roughness in Ra, S is spindle speed in rpm, F is feed rate mm/min and D is the diameter of the drill bit.

Trials	Experimental Result	Predicted Result	Predicted Value Error in %
1	337.29	332.96	1.284
2	324.58	321.33	1.0013
3	306	309.7	1.21
4	309.813	308.84	0.315
5	278.81	283.1	1.54
6	250.16	249.91	0.1
7	270.61	270.61	0
8	225.156	226.65	0.664

9	230.4	233.24	1.233
10	233.256	232.38	0.38
11	162.48	166.86	2.7
12	155.24	155.23	0.006
13	175.217	173.94	0.73
14	130.746	129.97	0.6
15	98.403	96.79	1.64
16	66.42	63.6	4.25

Table 4. 5: Experimental and predicted Values of surface roughness

The experimental and predicted values of surface roughness are shown in table 4.5. And also the predicted values are compared with the experimental value in the graph and shown below in the following Figure 4.3.

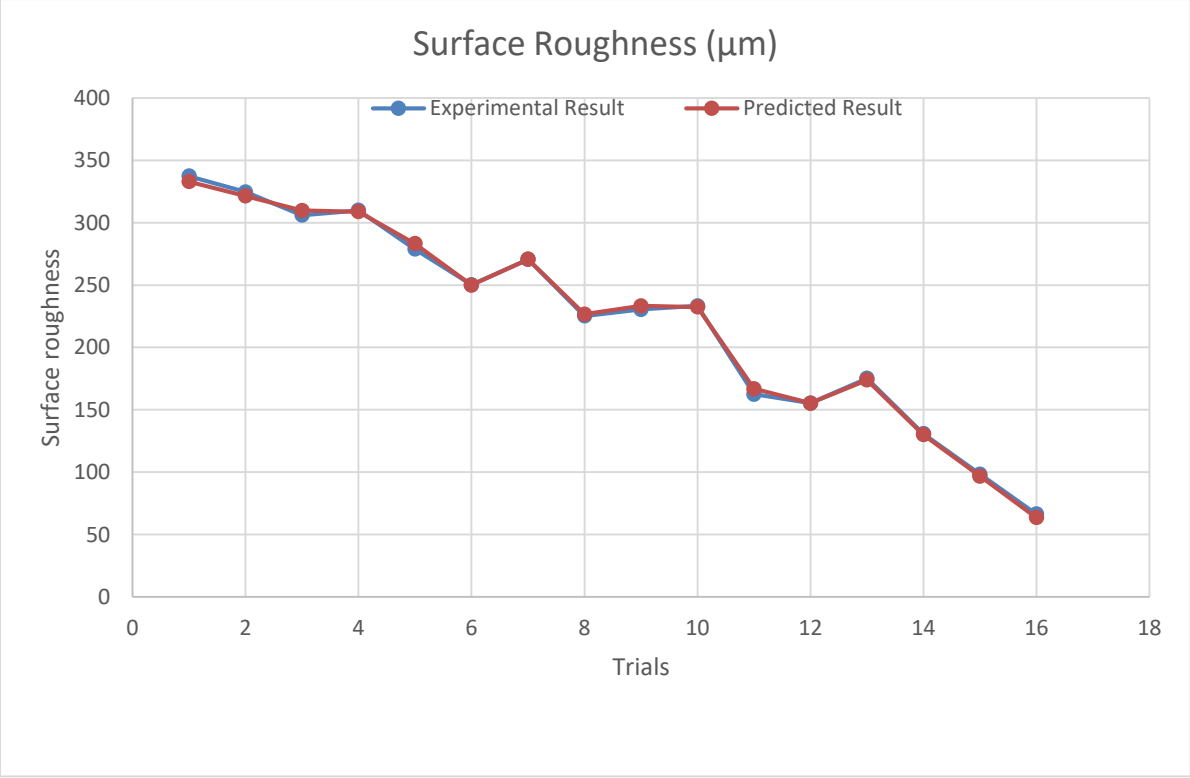

Figure 4. 3: Comparison of Experimental and Predicted values of surface roughness

4.3.2 The Signal to Noise Ratio Analysis

The term signal is the desirable value (mean) for the output characteristic in the Taguchi method, and the term noise is the undesired value (deviation, SD) for the output characteristic. The S / N ratio, therefore, is the average to SD ratio. Taguchi uses the S / N ratio to determine the quality attribute that deviates from the desired value. Depending on the type of characteristic, there are different S / N ratios available; lower the better, nominal the best, and higher the better [60,61].

Smaller the better (Eq. 4.2): is selected for this analysis because the desired surface roughness value should be the minimum value to obtain good surface finish of the hole.

So based on the surface roughness results (Table 4.6) the effect of the above parameters on the surface roughness of the drilled sample were analyzed using MINITAB 19 statistical software under Taguchi's analysis.

Experiment number	Spindle Speed (rpm)	Feed Rate (mm/min)	Drill diameter (mm)	Surface Roughness (µm)
1	600	10	6	337.290
2	600	15	7	324.580
3	600	20	8	306
4	600	25	10	309.813
5	900	10	7	278.810
6	900	15	6	250.160
7	900	20	10	270.610
8	900	25	8	225.156
9	1200	10	8	230.400
10	1200	15	10	233.256
11	1200	20	6	162.480

12	1200	25	7	155.240
13	1600	10	10	175.217
14	1600	15	8	130.746
15	1600	20	7	98.403
16	1600	25	6	66.420

Table 4. 6: L_{16} orthogonal array of spindle speed, feed rate, drill diameter, and surface roughness.

Using the data presented above with the formula chosen above (Eq. 4.2) to measure S / N ratio, the results of the Taguchi experiment are summarized in Table 4.6 and presented in Fig. 4.4, which was obtained using the statistical software MINITAB 19. From the S / N responses, it can be noted that spindle speed is the most significant factor influencing surface roughness since, as shown in Table 4.7 below, it is put in the first rank relative to other parameters based on signal to noise ratio analysis..

Response Table for Signal to Noise Ratios

Smaller is better

Level	Spindle Speed(rpm)	Feed Rate(mm/min)	Drill diameter(mm)
1	-50.09	-47.90	-44.79
2	-48.14	-46.95	-45.69
3	-45.66	-45.61	-46.58
4	-40.85	-44.28	-47.68
Delta	9.24	3.63	2.89
Rank	1	2	3

Table 4.7: Response table for the signal to noise ratio for surface roughness

Fig. 4.4 shows the effect of drilling parameters on surface roughness and the optimum values based on their rank. According to the overall analysis and the main effect plot for the SN ratio

graph shown below in Figure 4.4, the optimum values to minimize surface roughness are; 1600rpm, 25 mm/min, 6mm of spindle speed, feed rate, and drill diameter respectively.

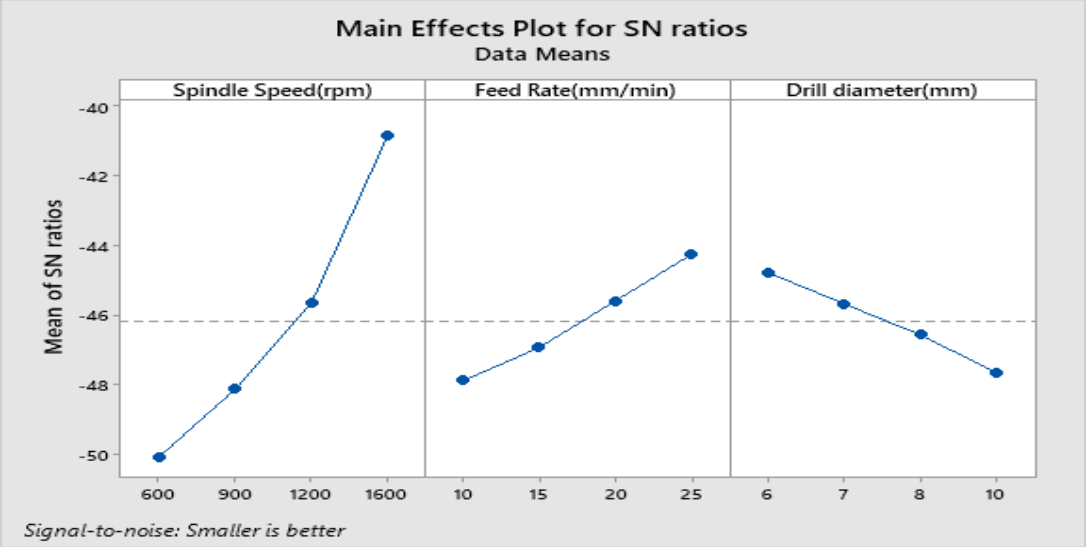

Figure 4. 4: Main effect plot for the mean of SN ratios of surface roughness

4.3.3 Analysis of Variance

A variance analysis (ANOVA) determines the relative significance of the factors concerning their percentage contribution to the reaction [60, 61]. For the valuation of the variance of error for the special effects and the confidence interval of the prediction of the error, ANOVA is also required. To acquire the percentage contribution of each of the parameters, the analysis is done based on their S / N ratios.

DF: Degree of freedom, SS: Sum of squares, Contribution: Contribution percentage, P-value: calculated probability, Adj MS: adjusted mean square, Adj SS: adjusted sum square, F-value: variance, Seq SS: sequential sum of squares with a confidence interval of 95 percent is obtained and displayed as follows in Table 4.8.

Analysis of Variance

Source	DF	Seq SS	Contribution	Adj SS	Adj MS	F-Value	P-Value
Spindle Speed(rpm)	3	89509	86.33%	89508.5	29836.2	5698.72	0.000
Feed Rate(mm/min)	3	10060	9.70%	10059.5	3353.2	640.46	0.000
Drill diameter(mm)	3	4083	3.94%	4083.1	1361.0	259.96	0.000
Error	6	31	0.03%	31.4	5.2		
Total	15	103683	100.00%				

Table 4. 8: ANOVA for the response of surface roughness

From table 4.8, observation can be made such that the spindle speed (86.33 percent) has a superior influence on surface roughness, and feed rate, drill diameter accounts 9.7 percent, and 3.94 percent contribution respectively on surface roughness. So from the above data, the p values are less than 0.05 for spindle speed this implies that spindle speed has a higher influence on the surface roughness during the drilling process.

4.4 Verification of Optimum Machining Parameters

Verification of the optimum machining parameters (spindle speed, feed rate, and drill diameter) to reduce roundness error and surface roughness based on the results from the analysis using Taguchi's method has been performed to verify the validation of the recommended optimum machining parameters. The selection of optimum machining parameter values to reduce both roundness error and surface roughness concurrently have seen all the analysis results. In the roundness error analysis, the optimum values to reduce roundness error are 600rpm, 15mm/min, and 6mm but drill diameter affects more than other parameters and it accounts for 96.49%. From this, we can deduce that spindle speed and feed rate impact to reduce roundness error are negligible because these parameters are dominated by drill diameter. On the other hand in the surface roughness analysis, the optimum values to reduce surface roughness are 1600rpm, 25mm/min, and 6mm but spindle speed and feed rate account for 86.33% and 9.7%. This shows

spindle speed and feed rate contributed 96% impact on the surface roughness and drill diameter have a very small effect on the surface roughness according to the analysis on the surface roughness.

So to reduce both roundness error and surface roughness based on the experimental analysis the optimum machining parameters that have been verified are 1600rpm, 25mm/min, and 6mm.

Four sample holes were drilled to verify the validation of the recommended optimum values using GMC CNC Milling Machine in METEC based on the part program generated by MASTERCAM X4 (APPENDIX E) with the same recommended spindle speed, feed rate, and drill diameter of 1600rpm, 25mm/min and 6mm respectively. Based on the verification experiment the verification results of roundness error and surface roughness values of four holes are shown below in Table 4.9 and 4.10 respectively.

- **Roundness error measurement values of four holes using recommended optimum drilling parameters (1600 rpm, 25 mm/min, and 6mm).**

First hole	Second hole	Third hole	Fourth hole
0.1	0.11	0.1	0.1

Table 4. 9: Roundness error values using optimum parameters

- **Surface roughness measurement values of four holes using recommended optimum drilling parameters (1600 rpm, 25 mm/min, and 6mm).**

Zeta Analysis Report
Image Name: Zeta Image File Name:
Date Acquired: Wed Nov 11 12:53:19 2020 Today: Wed Nov 11 12:53:33 2020
Z Range: 1100µm No. of Steps: 200 Step Size: 5.526µm Field of View: 1743µm x 1308µm

	Markers 1-2							
	Ra	Rq	Rpv	Rp	Rv	Rsk	Rz	Rku
	77.66	129.63	816.13	124.69	691.44	-2.956	389.21	13.31

(a)

Zeta Analysis Report
Image Name: Zeta Image File Name:
Date Acquired: Wed Nov 11 14:23:10 2020 Today: Wed Nov 11 14:23:15 2020
Z Range: 950µm No. of Steps: 200 Step Size: 4.773µm Field of View: 1743µm x 1308µm

	Markers 1-2							
	Ra	Rq	Rpv	Rp	Rv	Rsk	Rz	Rku
	51.88	81.48	573.04	70.54	502.5	-3.388	325.28	17.96

(b)

Zeta Analysis Report
Image Name: Zeta Image File Name:
Date Acquired: Wed Nov 11 14:13:12 2020 Today: Wed Nov 11 14:13:19 2020
Z Range: 502µm No. of Steps: 200 Step Size: 2.520µm Field of View: 1743µm x 1308µm

	Markers 1-2							
	Ra	Rq	Rpv	Rp	Rv	Rsk	Rz	Rku
	64.97	82.20	446.23	198.64	247.59	-0.6602	268.55	3.170

(c)

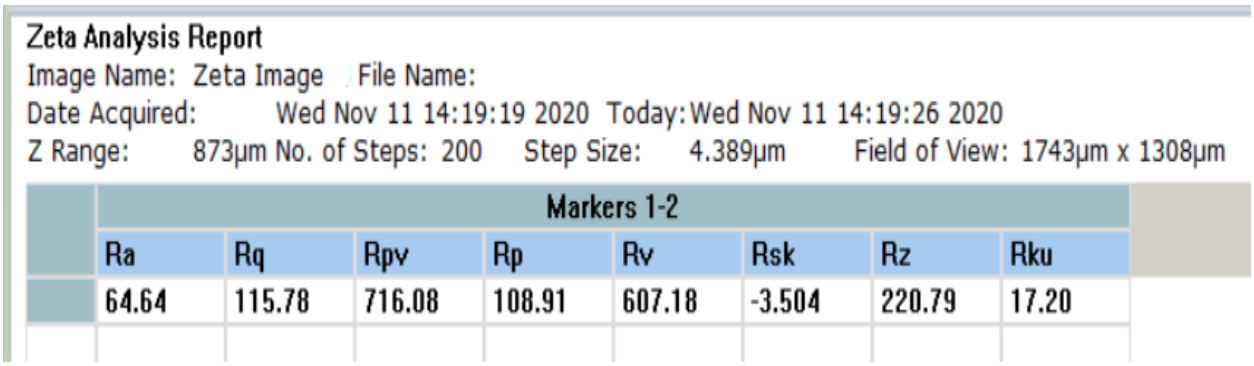

Zeta Analysis Report
Image Name: Zeta Image File Name:
Date Acquired: Wed Nov 11 14:19:19 2020 Today: Wed Nov 11 14:19:26 2020
Z Range: 873µm No. of Steps: 200 Step Size: 4.389µm Field of View: 1743µm x 1308µm

	Markers 1-2							
	Ra	Rq	Rpv	Rp	Rv	Rsk	Rz	Rku
	64.64	115.78	716.08	108.91	607.18	-3.504	220.79	17.20

(d)

Table 4. 10: Surface Roughness Values of the Four Holes (a,b,c,d)

In Conclusion, the experimental verification was performed based on the recommended **optimum machining parameters and drill diameter of the analysis** which are **1600 rpm, 25mm/min, and 6 mm** drill diameter respectively. The values of roundness error and surface roughness obtained are **0.1mm and 64.8 Ra**, which satisfies the objective of **lowest roundness error and surface roughness**. The verification result shows that the recommended machining parameter values to reduce roundness error and surface roughness based on Taguchi's analysis were precise and fitted to the optimum values.

CHAPTER FIVE

CONCLUSIONS AND RECOMMENDATIONS

5.1 Conclusions

This paper presents the optimization of machining parameters namely, spindle speed, feed rate, and drill diameter in drilling hybrid sisal-cotton fiber reinforced polyester composite using Taguchi's method of regression, signal-to-noise ratio, and ANOVA analysis. Drilling behaviors of fabricated composites were investigated based on different machining parameters and drill bits. The following are the conclusions based on the results of the experimental study.

- Using the L_{16} orthogonal array, statistically designed experiments built on the Taguchi method are performed to observe the influence of drilling parameters on roundness error and surface roughness.
- To calculate the values of roundness error and surface roughness, linear regression equations were generated and the measured values are compared with predicted values.
- According to the analysis and the main effect plot graph of signal to noise ratio the optimum values to reduce roundness error are; 600rpm, 15 mm/min, 6mm of spindle speed, feed rate, and drill diameter respectively.
- Also according to the analysis and the main effect plot graph of SN ratios the optimum values to reduce surface roughness are; 1600rpm, 25 mm/min, 6mm of spindle speed, feed rate, and drill diameter respectively.
- Based on ANOVA drill diameter (96.49%) has a superior influence on the roundness error compared to spindle speed (3.19%) and feed rate (0.25%).
- Through ANOVA Spindle speed (86.33%) and feed rate (9.7%) have a greater influence (96%) on the surface roughness compared to drill diameter (3.94%).
- From observations and verification of the experiment, the combination of the optimum values of the machining parameters and drill diameter for drilling HSCFRC laminates to reduce both roundness errors and surface roughnesses are 1600 rpm of spindle speed, 25 mm/min of feed rate, and 6 mm of drill diameter are preferred.

5.2 Recommendation for the Future Works

- From the author's point of view in this research, the author would like to recommend additional study could consider more factors such as drill properties (types of drills, point angle, number of flutes, and helix angle), run out of drill, torque, thrust force, tool wear, and material removal rate, etc. in the research to realize by what means these factors would distract the surface of drilled holes during the drilling process of the composite.

REFERENCES

[1] Saxena M, Murali S, Nandan MJ, et al, Sisal Potential for employment generation and rural development. In: 3rd International Conference Rural India, 2005, pp 208–212.

[2]. Rai A, Jha CN, Natural fiber composites and its potential as a building material. ExpressTextile, 25 Nov 2004.

[3]. Sharma D, India automotive components industry, Swiss Business Hub India, 2004, pp 1–20.

[4]. W. Hufenbach, Dobrzan ski LA, M. Gude, J. Koniezny, A. Czulak., "Optimization of rivet joints of CFRP composite material and aluminum alloy", *Journal of Achieves Materials and Manufacturing Engineering*, vol.20, 2007, pp. 119-122.

[5]. R. Teti, "*Machining of composite materials*", CIRP Annals – Manufacturing Technology, 51, 2002, pp.611-634.

[6]. R. Mirsha, J. Malik, I. Singh, J.P. Davim, " Neural network approach for estimate the residual tensile strength after drilling in unidirectional glass fiber reinforced plastic laminates" *Material Design*, 31,2010, pp.2790-2795.

[7].A. M Abrao, P.E Faria, J.C. Campos Rubio, P. Ries, J. P. Davim, "Drilling of fiber reinforced plastics: a review", *Journal of material processing Technology*, 186,2007, pp1-7.

[8] SP Systems. (2001). The advantages of epoxy resin versus polyester in marine composite structures, United Kingdom. Retrieved from http://www.mjmyachts.com/images/ stories/pdf/sp%20advantages%20of%20epoxy%20resin.pdf

[9] Singla, M. & Chawla, V., Mechanical Properties of Epoxy Resin – Fly Ash Composite. Journal of Minerals & Materials Characterization & Engineering, 2010, 9(3), 199 – 210.

[10] Hepworth, D. G., Hobson, R. N., Bruce, D. M., & Farrent, J. W., The use of unretted hemp fibre in composite manufacture. Composite Part A: Applied Science and Manufacturing, 2000, 31(11), 1279 – 1283.

[11] Mallick, P. K. 2008. Fibre-reinforcement composites, materials, manufacturing and

design. (3rd ed.). USA: CRC Press, Taylor and Francis Group, 2008.

[12] Kim, J. K., & Mai, Y. W. (1998). Engineered interfaces in fibre reinforced composites. (1st ed.). Oxford: Elsevier Science Ltd.

[13] Matthews, F. L., & Rawlings, R. D. (1994). Composite materials: Engineering and science. (1st ed.). Oxford: Chapman & Hall.

[14] Sridharan, S. (2008). Delamination behaviour of composites (1st ed.). Cambridge England: Woodhead Publishing Limited.

[15] Nirmal, U., Hashim, J., & Ahmed, M. M. H. M. (2015). A review on the tribological performance of natural fibre polymeric composites. Tribology International, 83, 77 – 104.

[16] Bagherpour, S. (2012). Polyester. In H. E. Salah (Ed.), Fiber reinforced polyester composites (pp. 135 – 166). Croatia: InTech.

[17] Liu, L., Jia, C., He, J., Zhao, F., Fan, D., Xing, L., Wang, M., Wang, F., Jiang, Z., & Yudong, H., (2015). Interfacial characterization, control and modification of carbon fiber reinforced polymer composites. Composites Science and Technology, 121, 1–38.

[18] Jawaid, M., & Abdul Khalil, H. P. S. (2011). Cellulosic/synthetic fibre reinforced polymer hybrid composites: A review. Carbohydrate Polymers, 86(1), 1-18.

[19] Terzopoulou, Z. N., Papageorgio, G. Z., Papadopoulou, E., Athanassiadou, E., Alexopoulou, E., & Bikiaris, D. N. (2015). Green composites prepared from aliphatic polyesters and bast fibers. Industrial Crops and Science, 68, 60 – 79.

[20] Kocsis, J., Mahmood, H., & Pegoretti, A. (2015). Recent advances in fiber/matrix interphase engineering for polymer composites. Progress in Materials Science, 73, 1–43.

[21] Shah, D. U. (2013). Developing plant fibre composites for structural applications by optimising composite parameters: a critical review. Journal of Material Science, 48, 6083-6107.

[22] Puglia, D., Biagiotti, J., & Kenny, J. M. (2004). application of natural reinforcements in composite materials, Part II: Application of natural reinforcements in composite materials for automotive industry. Journal of Natural Fibers, 1(3), 23 – 65.

[23] Sapuan, S. M., Kho, J. Y., Zainudin, E. S., Leman, Z., Ali, B. A. A., & Hambali, A. (2011). Material selection for natural fiber reinforced polymer composites using analytical hierarchy process. Indian Journal of Engineering and Materials Sciences, 18(4), 255 – 267.

[24] Cheung, H. Y., Ho, M. P., Lau, K. T., Cardona, F., & Hui, D. (2009). Natural fibre reinforced composites for bioengineering and environmental engineering applications. Composites Part B: Engineering, 40(7), 655 – 663.

[25] Graupner, N., Herrman, A. S., & Mussig, J. (2009). Natural and man-made cellulose fibre reinforced poly (lactic acid) (PLA) composites: An overview about mechanical characteristics and application areas, Composites Part A: Applied Science and Manufacturing, 40(6–7), 810 – 821.

[26] Ku, H., Wang, H., Pattarachaiyakoop, N., & Trada, M. (2011). A review on the tensile properties of natural fibre reinforced polymer composites. Composites Part B: Engineering, 42(4), 856-873.

[27] Pickering, K. (Ed.). (2008). Properties and performance of natural fibre composites. Boca Raton: CRC Press LLC.

[28] Wambua, P., Ivens, J., & Verpoest, I. (2003). Natural fibres: can they replace glass in fibre reinforced plastics. Composites Science and Technology, 63(9), 1259 – 1264.

[29] Faruk, O., Bledzki, A. K., Fink, H. P., & Sain, M. (2012). Biocomposites reinforced with natural fibers: 2000–2010. Progress in Polymer Science, 37(11), 1552-1596.

[30] Yan, Z., Zhang, J., Zhang, H., & Wang, H. (2013a). Improvement of mechanical propertiesof noil hemp fiber reinforced polypropylene composites by resin modification and fiber treatment. Advances in Materials Science and Engineering, 2013, 1-7.

[31] Kabir, M. M., Wang, H., Lau, K. T., & Cardona, F. (2012). Chemical treatments on plant based natural fibre reinforced polymer composites: An overview. Composites Part B: Engineering, 43(7), 2883 – 2892.

[32] Dhakal, H. N., Sarasini, F., Santulli, C., Tirillò, J., Zhang, Z., & Arumugam, V. (2015). Effect of basalt fibre hybridisation on post-impact mechanical behaviour of hemp fibre reinforced composites. Composites Part A: Applied Science and Manufacturing, 75, 54–67.

[33] Abiola, O. S., Kupolati, W. K., Sadiku, E. R., & Ndambuki, J. M. (2014). Utilisation of natural fibre as modifier in bituminous mixes: A review. Construction and Building Materials, 54, 305 – 312.

[34] Wang, H., Guo, Q., Yang, J., Liu, Z., Zhao, Y., Li, J., Feng, Z., & Liu, L. (2013). Microstructural evolution and oxidation resistance of polyacrylonitrile-based carbon fibers doped with boron by the decomposition of B4C. Carbon, 56, 296–308.

[35] Kopeliovich, D., (2012): Carbon fiber reinforced polymer composites. Substances and Technology. Retrieved from http://www.substech.com/dokuwiki/doku.php?id= carbon_fiber_reinforced_polymer_composites.

[36]. G.Dinesh, A.Guru Moorthy,and A.N.Balaji, "Mechanical and Corrosion Properties of Hybrid Sisal Fibre/Cotton Fibre/Coconut Sheath Reinforced Polymer Composites". www.mzcet.in › naac › documents; P. 275-.281.

[37]. KURT, M.; BAGCI, E.; KAYNAK, Y. (2009) "Application of Taguchi methods in the optimization of cutting parameters for surface finish and hole diameter accuracy in dry drilling processes" **International Journal of Advanced Manufacturing Technology**, v.40, n. 5-6, 2009, p. 458-469.

[38]. DAVIM, J. P.; REIS, P., Drilling carbon fiber reinforced plastic manufactured by auto clave experimental and statistical study, **Materials and Design,** v. 24, n. 5, 2003, p. 315-324.

[39]. KORKUT, I.; KUCUK, Y., Experimental Analysis of the Deviation from Circularity of Bored Hole Based on the Taguchi method. **Journal of Mechanical Engineering**, v. 56, n. 5, 2010, p. 340-346.

[40]. C.C. Tsao and H. Hocheng (2007) 'Evaluation of Thrust Force and Surface Roughness in Drilling Composite Material Using Taguchi Analysis and Neural Network' Elsevier - Journal of Materials Processing Technology.

[41]. Sahoo, P.; Barman, T.K.; Routara, B.C. "Fractal dimension modelling of surface profile and optimisation in CNC end milling using response surface method." Int. J. Manuf. Res. 2008, 3, 360–377.

[42] Hadi Rezghi Maleki , Mohsen Hamedi, Masatoshi Kubouchi and Yoshihiko Arao "Experimental study on drilling of jute fiber reinforced polymer composites", *Journal of Composite Materials*, 2018 p. 1–13.

[43] Taguchi G, Konishi S ,Taguchi Methods, orthogonal arrays and linear graphs, tools for quality American supplier institute, American Supplier Institute; 1987 p. 8-35.

[44] Rao, Ravella Sreenivas; C. Ganesh Kumar, R. Shetty Prakasham, Phil J. Hobbs, "The Taguchi Methodology as a statistical tool for biotechnological application: A critical appraisal", Biotechnology Journal 3 (4):510–523.

[45] Scarponi, C., Sarasini, F., Tirillo, J., Lampani, L., Valente, T., & Gaudenzi, P. (2015). Lowvelocity impact response of hemp fibre reinforced bio-based epoxy laminates, Proceedings of 5th Conference on Natural Fibre Composites for Industrial Applications, (pp. 1-4). Sapienza Universita de Roma, Rome: Italy.

[46] Faris, M. A., & Sapuan, S. M. (2014). Natural fiber reinforced polymer composites in industrial applications: feasibility of date palm fibers in sustainable automotive industry. Journal of Cleaner Production, 66, 347 – 354.

[47] Swoffs, Y., Gorbatikh, L., & Verpoest, I. (2014). Fibre hybridisation in polymer composites: A review. Composites Part A: Applied Science and Manufacturing, 67, 181–200.

[48] Ashby, M. F., & Cebon, D. (1992). Materials Selection in Mechanical Design. (4th ed.). Oxford: Pergamon Press.

[49] Klaus Fredric & Abdulhakim A. Almajid (2013), Manufacturing Aspects of Advanced Polymer Composites for Automotive Applications. Applied composite materials, 20(2013), 107-128.

[50] Ismail, S. O., Dhakal, H. N., Dimla, E., & Popov, I. (2016b). Recent advances in twist drill design for composites machining: A critical review, Proceedings of the Institution of Mechanical Engineers, Part B: Journal of Engineering Manufacture, 1-16.

[51] Astakhov, V. P., & Davim, J. P. (2008). Tools (geometry and material) and tool wear. In J. P. Davim (Ed.), Machining fundamentals and recent advances (pp. 29-57). USA: Springer.

[52] Liu, D. F., Tang, Y. J., & Cong, W. L. (2012). A review of mechanical drilling for composite laminates. Composite Structures, 94(4), 1265–1279.

[53] Hocheng, H., & Tsao, C. C. (2003). Comprehensive analysis of delamination in drilling of composite materials with various drill bits. Journal of Materials Processing Technology, 140(1-3), 335-339.

[54] Davim, J. P., & Reis, P. (2003a). Study of delamination in drilling carbon fibre reinforced plastics (CFRP) using design experiments. Composite Structures, 59(4), 481-487.

[55] Che, W. (1997). Some experimental investigations in the drilling of carbon fibre-reinforced plastic (CFRP) composite laminates. International Journal of Machine Tools and Manufacture, 37(8), 1097-1108.

[56] Garrick, R. (2007). Drilling advanced aircraft structures with PCD (Poly-Crystalline Diamond) drills. SAE International Technical Paper, pp.1-9.

[57] Madhavan, S., & Prabu, S. B. (2012). An experimental study of influence of drill geometry on drilling of carbon fibre reinforced plastic composites. International Journal of Engineering Research and Development, 3(1), 36-44.

[58] Faraz, A., Biermann, D., & Weinert, K. (2009). Cutting edge rounding: An innovative tool wear criterion in drilling CFRP composite laminates. International Journal of Machine Tools and Manufacture, 49(15), 1185-1196.

[59] Makhdum, F., Phadnis, V. A., Roy, A., & Silberschmidt, V. V. (2014). Effect of ultrasonicallyassisted drilling on carbon-fibre-reinforced plastics. Journal of Sound and Vibration, 333(23), 5939–5952.

[60] Philip J Ross (1996) Taguchi techniques for quality engineering, McGraw-Hill

[61] Phadke M S (1989) Quality engineering using robust design, Prentice Hall, Englewood Cliffs, NJ.

[62] Sikiru Oluwarotimi ISMAIL, Machinability Analysis of Drilling Induced Damage on Fiber-Reinforced Polymer Composites, University of Portsmouth, 2017, 4-68.

[63] Keyence Corporation of America: Measuring Roundness Error, 2021, retrieved from

https://www.keyence.com/ss/products/measure-sys/gd-and-t/form-tolerance/roundness.jsp

APPENDIX A

Sample 1 surface roughness test results of 16 holes using Zeta 20 profilometer is summarized in the following table as follows:

Table A: Sample 1 Surface Roughness Results

Table A.1: Sample 1 hole 1 Test results

Ra	Rq	Rpv	Rp	Rv	Rsk	Rz	Rku
325.56	370.61	1568.57	619.06	949.51	-0.2446	801.91	2.073

Table A.2: Sample 1 hole 2 Test results

Ra	Rq	Rpv	Rp	Rv	Rsk	Rz	Rku
347.44	396.60	1404.88	506.92	897.96	-0.5736	523.53	2.163

Table A.3: Sample 1 hole 3 Test results

Ra	Rq	Rpv	Rp	Rv	Rsk	Rz	Rku
300.15	336.44	1174.35	656.38	517.98	0.2601	839.74	1.821

Table A.4: Sample 1 hole 4 Test results

Ra	Rq	Rpv	Rp	Rv	Rsk	Rz	Rku
313.91	396.49	1702.08	713.12	988.96	-0.5699	1386.21	2.668

Table A.5: Sample 1 hole 5 Test results

Ra	Rq	Rpv	Rp	Rv	Rsk	Rz	Rku
286.77	353.31	1759.04	648.99	1110.05	-0.3321	1184.24	2.640

Table A.6: Sample 1 hole 6 Test results

Ra	Rq	Rpv	Rp	Rv	Rsk	Rz	Rku
255.46	306.69	1365.29	635.25	730.04	-0.2241	663.4	2.468

Table A.7: Sample 1 hole 7 Test results

Ra	Rq	Rpv	Rp	Rv	Rsk	Rz	Rku
270.75	332.10	1504.79	606.26	898.53	-0.2669	923.80	2.477

Table A.8: Sample 1 hole 8 Test results

Ra	Rq	Rpv	Rp	Rv	Rsk	Rz	Rku
227.45	265.87	1044.50	443.23	601.26	-0.2587	558.50	1.995

Table A.9: Sample 1 hole 9 Test results

Ra	Rq	Rpv	Rp	Rv	Rsk	Rz	Rku
227.56	272.11	1124.13	455.45	668.68	-0.5877	609.4	2.593

Table A.10: Sample 1 hole 10 Test results

Ra	Rq	Rpv	Rp	Rv	Rsk	Rz	Rku
233.33	282.80	1238.77	528.02	710.75	-0.6176	747.16	2.744

Table A.11: Sample 1 hole 11 Test results

Ra	Rq	Rpv	Rp	Rv	Rsk	Rz	Rku
169.91	197.78	722.59	253.04	469.56	-0.4893	450.48	2.180

Table A.12: Sample 1 hole 12 Test results

Ra	Rq	Rpv	Rp	Rv	Rsk	Rz	Rku
157.01	193.18	835.85	406.08	429.78	-0.3074	519.98	2.549

Table A.13: Sample 1 hole 13 Test results

Ra	Rq	Rpv	Rp	Rv	Rsk	Rz	Rku
175.15	207.92	877.3	451.82	425.50	-0.2763	628.86	2.178

Table A.14: Sample 1 hole 14 Test results

Ra	Rq	Rpv	Rp	Rv	Rsk	Rz	Rku
133.93	162.00	729.69	359.95	369.74	-0.3056	564.76	2.507

Table A.15: Sample 1 hole 15 Test results

Ra	Rq	Rpv	Rp	Rv	Rsk	Rz	Rku
98.91	116.05	470.76	184.71	286.05	-0.2332	350.36	2.101

Table A.16: Sample 1 hole 16 Test results

Ra	Rq	Rpv	Rp	Rv	Rsk	Rz	Rku
70.47	84.08	409.45	190.56	218.89	-0.1701	302.50	2.328

APPENDIX B

Sample 2 surface roughness test results of 16 holes using Zeta 20 profilometer is summarized in the following table as follows:

Table B: Sample 2 Surface Roughness Results

Table B.1: Sample 2 hole 1 Test results

Ra	Rq	Rpv	Rp	Rv	Rsk	Rz	Rku
328.49	372.87	1577.7	623.46	954.23	-0.2316	825.40	2.065

Table B.2: Sample 2 hole 2 Test results

Ra	Rq	Rpv	Rp	Rv	Rsk	Rz	Rku
337.65	387.58	1392.46	486.14	906.32	-0.5935	597.32	2.234

Table B.3: Sample 2 hole 3 Test results

Ra	Rq	Rpv	Rp	Rv	Rsk	Rz	Rku
306.19	342.83	1191.63	663.83	527.79	0.2434	860.02	1.797

Table B.4: Sample 2 hole 4 Test results

Ra	Rq	Rpv	Rp	Rv	Rsk	Rz	Rku
309.30	392.03	1683.10	708.37	974.72	-0.5646	1334.97	2.689

Table B.5: Sample 2 hole 5 Test results

Ra	Rq	Rpv	Rp	Rv	Rsk	Rz	Rku
270.75	332.10	1504.79	606.26	898.53	-0.2669	923.80	2.477

Table B.6: Sample 2 hole 6 Test results

Ra	Rq	Rpv	Rp	Rv	Rsk	Rz	Rku
249.78	298.58	1315.84	610.93	704.92	-0.2680	561.96	2.462

Table B.7: Sample 2 hole 7 Test results

Ra	Rq	Rpv	Rp	Rv	Rsk	Rz	Rku
273.05	335.10	1541.06	612.62	928.44	-0.2755	952.35	2.494

Table B.8: Sample 2 hole 8 Test results

Ra	Rq	Rpv	Rp	Rv	Rsk	Rz	Rku
222.33	260.42	1021.90	428.31	593.60	-0.2495	496.55	1.998

Table B.9: Sample 2 hole 9 Test results

Ra	Rq	Rpv	Rp	Rv	Rsk	Rz	Rku
230.31	276.60	1165.84	486.13	679.70	-0.6078	665.61	2.659

Table B.10: Sample 2 hole 10 Test results

Ra	Rq	Rpv	Rp	Rv	Rsk	Rz	Rku
237.98	295.35	1379.25	594.36	784.9	-0.5993	798.94	2.918

Table B.11: Sample 2 hole 11 Test results

Ra	Rq	Rpv	Rp	Rv	Rsk	Rz	Rku
162.45	191.03	686.38	244.87	441.51	-0.4950	345.09	2.257

Table B.12: Sample 2 hole 12 Test results

Ra	Rq	Rpv	Rp	Rv	Rsk	Rz	Rku
155.03	191.00	828.13	407.51	420.61	-0.3080	490.84	2.561

Table B.13: Sample 2 hole 13 Test results

Ra	Rq	Rpv	Rp	Rv	Rsk	Rz	Rku
181.33	215.30	927.79	470.59	457.20	-0.2369	710.12	2.170

Table B.14: Sample 2 hole 14 Test results

Ra	Rq	Rpv	Rp	Rv	Rsk	Rz	Rku
130.65	157.3	705.68	347.85	357.82	-0.3042	544.35	2.470

Table B.15: Sample 2 hole 15 Test results

Ra	Rq	Rpv	Rp	Rv	Rsk	Rz	Rku
100.16	128.63	516.14	172.39	343.76	-0.9937	225.60	3.420

Table B.16: Sample 2 hole 16 Test results

Ra	Rq	Rpv	Rp	Rv	Rsk	Rz	Rku
66.33	79.81	356.46	180.48	175.99	-0.1114	264.08	2.243

APPENDIX C

Sample 3 surface roughness test results of 16 holes using Zeta 20 profilometer is summarized in the following table as follows:

Table C: Sample 3 Surface Roughness Results

Table C.1: Sample 3 hole 1 Test results

Ra	Rq	Rpv	Rp	Rv	Rsk	Rz	Rku
319.69	364.45	1549.86	606.89	942.97	-0.2701	844.95	2.100

Table C.2: Sample 3 hole 2 Test results

Ra	Rq	Rpv	Rp	Rv	Rsk	Rz	Rku
326.78	378.5	1335.9	457.47	878.39	-0.6282	542.60	2.284

Table C.3: Sample 3 hole 3 Test results

Ra	Rq	Rpv	Rp	Rv	Rsk	Rz	Rku
311.61	348.72	1209.02	669.72	539.31	0.2253	878.89	1.777

Table C.4: Sample 3 hole 4 Test results

Ra	Rq	Rpv	Rp	Rv	Rsk	Rz	Rku
306.23	388.82	1670.88	709.57	961.31	-0.5566	1305.77	2.690

Table C.5: Sample 3 hole 5 Test results

Ra	Rq	Rpv	Rp	Rv	Rsk	Rz	Rku
278.91	342.68	1635.1	626.41	1008.70	-0.2930	1069.33	2.543

Table C.6: Sample 3 hole 6 Test results

Ra	Rq	Rpv	Rp	Rv	Rsk	Rz	Rku
245.26	291.49	1270.38	591.25	679.13	-0.2887	572.90	2.438

Table C.7: Sample 3 hole 7 Test results

Ra	Rq	Rpv	Rp	Rv	Rsk	Rz	Rku
268.03	329.04	1470.68	600.45	870.23	-0.2689	893.23	2.479

Table C.8: Sample 3 hole 8 Test results

Ra	Rq	Rpv	Rp	Rv	Rsk	Rz	Rku
225.69	263.92	1037.42	440.07	597.34	-0.2542	535.6	1.992

Table C.9: Sample 3 hole 9 Test results

Ra	Rq	Rpv	Rp	Rv	Rsk	Rz	Rku
233.33	282.80	1238.77	528.02	710.75	-0.6176	747.16	2.744

Table C.10: Sample 3 hole 10 Test results

Ra	Rq	Rpv	Rp	Rv	Rsk	Rz	Rku
228.46	273.64	1138.47	464.56	673.91	-0.5956	628.80	2.615

Table C.11: Sample 3 hole 11 Test results

Ra	Rq	Rpv	Rp	Rv	Rsk	Rz	Rku
155.08	183.41	659.84	240.40	419.44	-0.4926	315.74	2.339

Table C.12: Sample 3 hole 12 Test results

Ra	Rq	Rpv	Rp	Rv	Rsk	Rz	Rku
153.26	188.98	830.63	410.80	419.82	-0.2994	475.46	2.579

Table C.13: Sample 3 hole 13 Test results

Ra	Rq	Rpv	Rp	Rv	Rsk	Rz	Rku
169.14	200.40	851.76	443.07	408.69	-0.2848	662.67	2.210

Table C.14: Sample 3 hole 14 Test results

Ra	Rq	Rpv	Rp	Rv	Rsk	Rz	Rku
127.66	153.13	682.21	335.6	346.65	-0.2966	523.67	2.426

Table C.15: Sample 3 hole 15 Test results

Ra	Rq	Rpv	Rp	Rv	Rsk	Rz	Rku
96.14	123.26	494.68	166.18	328.49	-0.9841	250.81	3.350

Table C.16: Sample 3 hole 16 Test results

Ra	Rq	Rpv	Rp	Rv	Rsk	Rz	Rku
62.45	75.37	322.90	167.51	155.4	-0.1334	230.22	2.229

APPENDIX D

The part programs used to drill the sample based on Taguchi's L_{16} orthogonal array matrix are listed below.

The part program for 6mm drill bit;

O1115

N100 G21

N102 G0 G17 G40 G49 G80 G90

N106 G0 G90 G54 X-45.71 Y19.25 S600 M3

N108 G43 H1 Z25.

N110 G99 G73 Z-6. R25. Q1. F10.

N112 G80

N114 S900 M3

N116 X-27.42

N118 G99 G73 Z-6. R25. Q1. F15.

N120 G80

N122 S1200 M3

N124 X-9.13

N126 G99 G73 Z-6. R25. Q1. F20.

N128 G80

N130 S1600 M3

N132 X9.16

N134 G99 G73 Z-6. R25. Q1. F25.

N136 G80

N138 M5

N140 G91 G28 Z0.

N142 G28 X0. Y0.

N144 M30

%

Part program for 7 mm diameter drill diameter;

O1116

N100 G21

N102 G0 G17 G40 G49 G80 G90

N106 G0 G90 G54 X27.45 Y19.25 S600 M3

N108 G43 H2 Z25.

N110 G99 G73 Z-6. R25. Q1. F15.

N112 G80

N114 S900 M3

N116 X45.74

N118 G99 G73 Z-6. R25. Q1. F10.

N120 G80

N122 S1200 M3

N124 Y0.

N126 G99 G73 Z-6. R25. Q1. F25.

N128 G80

N130 S1600 M3

N132 X27.45

N134 G99 G73 Z-6. R25. Q1. F20.

N136 G80

N138 M5

N140 G91 G28 Z0.

N142 G28 X0. Y0.

N144 M30

%

Part program for 8mm diameter drill bit;

O1117

N100 G21

N102 G0 G17 G40 G49 G80 G90

N106 G0 G90 G54 X-45.71 Y0. S600 M3

N108 G43 H3 Z25.

N110 G99 G73 Z-6. R25. Q1. F20.

N112 G80

N114 S900 M3

N116 X-27.42

N118 G99 G73 Z-6. R25. Q1. F25.

N120 G80

N122 S1200 M3

N124 X-9.13

N126 G99 G73 Z-6. R25. Q1. F10.

N128 G80

N130 S1600 M3

N132 X9.16

N134 G99 G73 Z-6. R25. Q. F15.

N136 G80

N138 M5

N140 G91 G28 Z0.

N142 G28 X0. Y0.

N144 M30

%

Part program for 10mm diameter drill bit;

O1118

N100 G21

N102 G0 G17 G40 G49 G80 G90

N106 G0 G90 G54 X-45.71 Y-19.25 S600 M3

N108 G43 H4 Z25.

N110 G99 G73 Z-6. R25. Q1. F25.

N112 G80

N114 S900 M3

N116 X-27.42

N118 G99 G73 Z-6. R25. Q1. F20.

N120 G80

N122 S1200 M3

N124 X-9.13

N126 G99 G73 Z-6. R25. Q1. F15.

N128 G80

N130 S1600 M3

N132 X9.16

N134 G99 G73 Z-6. R25. Q1. F10.

N136 G80

N138 M5

N140 G91 G28 Z0.

N142 G28 X0. Y0.

N144 M30

%.

APPENDIX E

Part programs for verification of the recommended optimum drilling parameters;

O2215

N100 G21

N102 G0 G17 G40 G49 G80 G90

N106 G0 G90 G54 X-45.71 Y19.25 S1600 M3

N108 G43 H1 Z25.

N110 G99 G73 Z-6. R25. Q1. F25.

N112 G80

N114 S1600 M3

N116 X-27.42

N118 G99 G73 Z-6. R25. Q1. F25.

N120 G80

N122 S1600 M3

N124 X-9.13

N126 G99 G73 Z-6. R25. Q1. F25.

N128 G80

N130 S1600 M3

N132 X9.16

N134 G99 G73 Z-6. R25. Q1. F25.

N136 G80

N138 M5

N140 G91 G28 Z0.

N142 G28 X0. Y0.

N144 M30

%